INTERNATIONAL JOURNAL OF CLIMATOLOGY
Int. J. Climatol. **27**: 1303–1325 (2007)
Published online 7 February 2007 in Wiley InterScience
(www.interscience.wiley.com) DOI: 10.1002/joc.1473

RMetS
ROYAL METEOROLOGICAL SOCIETY

Characteristics of US drought and pluvials from a high-resolution spatial dataset

Ryan S. Kangas and Timothy J. Brown*
Desert Research Institute, Reno, Nevada, USA

Abstract:

Anomalous precipitation can be a devastating natural disaster having significant impacts on economies, society and the environment. This study examines the spatial and temporal characteristics of anomalous precipitation throughout the United States to obtain a greater understanding of drought/pluvial regimes, including intensity, duration and spatial coverage based on a high-resolution precipitation dataset. With the help of the parameter-elevation regression on independent slopes model (PRISM), approximately 4 km data for the United States is used to construct the Palmer drought severity index (PDSI) and the standardized precipitation index (SPI) for the period 1895–2003. Increased resolution from the PRISM dataset shows that drought/pluvial areas are not as homogeneous as seen in previous studies based on climate divisions and larger scales. While size, duration and locations of drought/pluvial events are influenced by the index used, the largest annual drought/pluvial events occur more frequently in the central United States, with a higher percentage of extreme values occurring in the western portion of the country. Four large pluvial events have occurred in the United States during the study period, with three of these having occurred during the past 30 years. Copyright © 2007 Royal Meteorological Society

KEY WORDS drought; pluvial; Palmer drought severity index; standardized precipitation index; PRISM; gridded precipitation

Received 17 February 2006; Revised 3 November 2006; Accepted 4 November 2006

INTRODUCTION

The effects of anomalous precipitation regimes are felt physically, economically, socially and politically, and are one of the most persistent, naturally occurring climate-related hazards to impact societies throughout most of the populated world. Droughts impact both surface and groundwater resources and can lead to reductions in water supply, diminished water quality, crop failure, reduced range productivity, diminished power generation, disturbed riparian habitats and suspended recreation activities, as well as a host of other economic and social activities (Riebsame *et al*., 1991). On the other hand, prolonged wet periods can lead to ruined harvest from flooded fields, and can cause rivers to overflow their banks, flooding cities and destroying property (Diaz, 1983).

Throughout history, droughts have been responsible for declines in civilization and have caused many to migrate to more prosperous lands. Proxy climate records suggest that a century scale decline in precipitation from A.D. 800 to 900 may have stressed resources and contributed to social stresses, leading to the Mayan demise (Haug *et al*., 2003). Drought may have led to the fall of Andean civilizations in late A.D. 1100, the Mediterranean during the Late Bronze Age, and in fact throughout recorded history (Weiss, 1981; Binford *et al*., 1997).

Recent examples of the devastating effects of drought on society are not hard to find. During the 1930s and 1950s, the Great Plains essentially dried up during the most severe droughts in instrumental history, causing massive migrations throughout much of the United States (Fye *et al*., 2003; Hidalgo, 2004). Likewise, a substantial pluvial event in the early 20th century (1905–1917) lasted for over a decade and led to bias estimates of stream discharge in the Colorado River basin, and contributed to an unrealistic allocation of water for the coming decades (Fye *et al*., 2003). The Great Plains and the western United States are particularly prone to anomalous precipitation regimes, and are becoming increasingly more vulnerable due to changes including large population growths and farming of marginal lands (Diaz, 1983). Estimates are poor for the return frequency of severe droughts such as that of the 1930s, ranging from 75 to 3000 years (Yevjevich, 1967; Bowden *et al*., 1981).

The instrumental record of the past 100 years represents only a small subset of historical drought. Droughts of the 20th century in the United States have been eclipsed several times in the past 2000 years both spatially and temporally (Woodhouse and Overpeck, 1998), while there have been at least three past pluvial events comparable to the early 20th century pluvial (Fye *et al*., 2003). With the use of paleoclimatic reconstructions, Bark (1978) concludes that since the 13th century there have been at least 12 droughts lasting more then 10 years,

* Correspondence to: Timothy J. Brown, 2215 Raggio Parkway, Reno, Nevada, 89512, USA. E-mail: tim.brown@dri.edu

3 lasting longer than 20 years, with the longest lasting 38 years near the end of the 13th century. By comparison, the droughts of the 1930s and 1950s only lasted approximately 10 years (Diaz, 1983). However, Fye *et al*. (2003) believe that, in terms of intensity, duration and coverage, the 1930s drought was the worst since the 1700s with 1934 being the most extreme year in 300 to possibly 500 years.

Past examinations of spatial and temporal extents of drought have been numerous (e.g., Skaggs, 1975; Klugman, 1978; Karl, 1983; McGregor, 1985; Oladipo, 1986; Soulé and Meentemeyer, 1989), while examinations of wet periods have been fewer in number (e.g., Diaz, 1983; Fye *et al*., 2003). Fye *et al*. (2003) indicated that during the past 500 years only three pluvials may have equaled that of the early 20th century occurring from 1549–1558, 1602–1622 and 1825–1840. One of the most consistent findings amongst these studies is the greater likelihood and persistence of prolonged periods of anomalous moisture regimes in the interior and western United States based upon the PDSI (Karl and Koscielny, 1982; Walsh *et al*., 1982, Diaz, 1983; Karl, 1983; Karl *et al*., 1987; Hidalgo, 2004).

Much of drought research has focused on meteorological, hydrologic and agricultural characteristics and impacts, but there has been minimal emphasis on forest and ecosystem impacts. The present study was done in part to provide a high-resolution drought/pluvial analysis for land managers. Both drought and wet periods can lead to a variety of land management issues. The primary response to drought is the mortality of small structure plants; however, severe and prolonged droughts also render mature trees susceptible to insect infestations and disease adding to vegetation mortality (Allen and Breshears, 1998; Hanson and Weltzin, 2000). Drought conditions can also lead to a decrease in decomposition (Dale *et al*., 2001). This, along with the increased vegetation mortality, can lead to a buildup of dry fuels resulting in large and severe wildfires. Precipitation and temperature on several temporal scales (seasonal, annual, decadal and centennial) regulate biomass production and control the conditioning of fuels.

Drought can be responsible for shifts in ecotones. Allen and Breshears (1998) document an extensive ecotone shift in northern New Mexico during the 1950's drought, where mortality of ponderosa pine, due to drought and insects, led to a shift toward pinyon-juniper woodlands. In the coming decades, climate changes are expected to produce similar shifts in vegetation at unprecedented rates (Allen and Breshears, 1998). Recent simulations of climate change effects in California indicate a shift in dominance from needle-leaved to broad-leaved plants and an overall increase in vegetation biomass with increasing temperatures (Lenihan *et al*., 2003). Vegetation change due to precipitation is more complex given soil moisture characteristics and tree–grass interactions due to fire. Their conclusions also indicated that any changes in fire regimes are less likely to be from altered fire weather and more from changes in the amount and types of fuels.

A positive precipitation anomaly affects management of lands by increasing vegetation biomass and fine fuel loads. Rogers and Vint (1987) showed that more acres were burned in the Arizona Sonoran desert following two winters of above-normal precipitation. Above-normal seed reserves from the first wet winter resulted in an increased biomass load following the second winter. Swetnam and Betancourt (1998) also found that while severe fire years are associated with drought, antecedent moisture conditions affect fine fuel production 1 to 3 years prior to large fires in ponderosa pine forests. A 1-year lag may reflect grass production, and a 2 or 3 years lag the buildup of needle litter. While insect outbreaks are usually associated with drought conditions, a 300-year reconstruction of western spruce budworm outbreaks in the central and southern Rockies of Colorado and New Mexico indicate that budworm outbreaks generally occur during wet periods. This example shows that some bud- and leaf-feeding insects have enhanced food quality and quantity with increased moisture (Swetnam and Betancourt, 1998).

The primary purpose of this study is to examine the spatial and temporal coverage of anomalous precipitation regimes using short- to long-term timescales and multiple drought indices based on a historical high-resolution gridded dataset. The basis for much of this analysis is from Soulé (1992); however, attention here is given to greater spatial resolution, a number of different indices and a focus on both positive and negative precipitation anomalies. Two index types will be used – the PDSI (Palmer, 1965) and the standardized precipitation index (McKee *et al*., 1993). Attributes of both indices are well discussed in Heim (2002) and summarized in the data section below. The PDSI is included here given its long history and widespread use. The SPI is used in part for its simplicity, as it is only dependant on precipitation and is easily modified for various timescales.

There are three questions addressed in this study: (1) how do various timescales and indices affect spatial patterns of frequency and duration? (2) how does increased spatial resolution compare with coarser scales such as climate divisions? and (3) what are the spatial and temporal patterns of anomalous precipitation, given a high-resolution dataset?

DATA AND METHODS

Parameter-elevation regression on independent slopes model (PRISM)

PRISM is a climate analysis system that uses point data, a digital elevation model (DEM) at 2.5-min latitude–longitude grid spacing and other spatial datasets to generate gridded estimations of annual, monthly and event-based climatic parameters (Daly *et al*., 1997). PRISM is unique in that it incorporates a spatial climate knowledge base that accounts for rain shadows, temperature inversions, coastal effects, high mountains

DOI: 10.1002/joc

and other complex regimes in the climate-mapping process (Daly *et al*., 1994). It is well suited to regions of mountainous terrain because it incorporates a conceptual framework that addresses the spatial scale and patterns of orographic precipitation. While originally developed in 1991 for precipitation estimates, it has since been applied to maximum and minimum temperature, snowfall and other climate elements.

PRISM determines climate by calculating linear relationships between climate elements, in particular precipitation and elevation. Each grid cell value is calculated by a separate regression function using data from nearby stations. Each station included in the multiple regression is weighted on five factors: distance, elevation, vertical layer, topographic facet and coastal proximity. The PRISM products underwent a rigorous peer-reviewed process that resulted in many significant enhancements. Further details can be found at [http://www.ocs.orst.edu/prism/docs/index.phtml] (October 2006).

PRISM temperature and precipitation data for 1895–1999 were acquired from [http://www1.ncdc.noaa.gov/pub/data/prism100] (October 2006), and for 2000–2003 via the Oregon State University Spatial Climate Analysis Service (SCAS) web site [http://www.ocs.orst.edu/prism] (December 2006). These data were used in the calculation of an approximate 4-km resolution SPI and PDSI monthly values for the conterminous United States. Each month for the 1895–2003 period had 451 709 grid points. This number times the 14 indices yielded over 8.2 billion grid point calculations.

Palmer drought severity index (PDSI)

The most widely used drought index in the United States is the PDSI, developed by Palmer (1965). He recognized the need for a better monitoring tool that could identify droughts in terms of their intensity, duration and spatial extent (Hayes *et al*., 1999). The Palmer indices are widely accepted by climatologists as representative measures of drought, and have been calculated as the main national drought indices for over 30 years. While there has been discussion on the utility of the PDSI and its limited success as a drought-monitoring tool (Hayes *et al*., 1999), it was chosen for this analysis because of its continued popularity.

There are three variations of the index today: Palmer Modified Drought Index (PMDI) designed for real-time use, Palmer hydrologic drought index (PHDI) designed for water supply monitoring and the Z-index (ZINX), which is the measure of an individual month's wetness or dryness. Each of these variations shares many characteristics with the original PDSI. In this study, only the PDSI is examined.

The Palmer index is based on the concept of anomalies in the supply and demand of the water balance equation. The calculations involved in the PDSI are quite complex; Palmer (1965) identifies 68 terms involved in creating the final output. The inputs include precipitation, temperature, evapotranspiration (based on Thornthwaite's work), soil moisture and latitude. The data are standardized to account for regional differences; therefore, the index should be a similar representation for differing areas even though the actual rainfall deficiencies vary (Hayes *et al*., 1999). The software code for computing Palmer indices is available from the National Climatic Data Center (NCDC) at [http://www.ncdc.noaa.gov/pub/software/palmer/pdi.f] (October 2006).

The limitations of the PDSI have been documented in several papers (Alley, 1984; Karl and Knight, 1985; Willeke, 1994; McKee *et al*., 1995; Guttman, 1997). Limits of the PDSI include the following: (1) an inherent timescale making the PDSI more suited for agricultural impacts and not so much for hydrologic and (2) assumptions that all precipitation is rain, thus making values during winter months and high elevations often questionable. PDSI also assumes that runoff only occurs after all soil layers have become saturated, leading to an underestimation of runoff.

According to Hayes *et al*. (1999), PDSI can be slow to respond to developing and diminishing droughts. The PDSI has also been criticized for responding too slowly to agricultural drought (Steila, 1972) and too quickly to hydrologic drought (Alley, 1985). Karl (1983, 1986) and Alley (1984) detail further procedures and limitations of the PDSI. While there are some criticisms of the PDSI, there are positive aspects as well. The PDSI has been in use for a long time, and has been well tested and verified in many cases. The PDSI accounts for temperature and soil characteristics, and is standardized so comparisons of different climates are possible. The adjective classifications of the index values are given in Table I.

PDSI soil data

PDSI requires soil information (available water content) as a parameter input. Available water capacity is defined in the Natural Resource Conservation Service (NRCS) Soil Survey Manual as "the volume of water that should be available to plants if the soil, inclusive of rock fragments, were at field capacity." For the present study, the required soil water content data was obtained from the

Table I. PDSI index values and adjective classifications.

Value	Class
$\geq$4.00	Extremely wet
3.00 to 3.99	Very wet
2.00 to 2.99	Moderately wet
1.00 to 1.99	Slightly wet
0.50 to 0.99	Incipient wet spell
0.49 to −0.49	Near normal
−0.50 to −0.99	Incipient drought
−1.00 to −1.99	Mild drought
−2.00 to −2.99	Moderate drought
−3.00 to −3.99	Severe drought
≤ -4.00	Extreme drought

DOI: 10.1002/joc

Earth Systems Science Center in the College of Earth and Mineral Sciences at the Pennsylvania State University [http://www.soilinfo.psu.edu/index.cgi] (October 2006). Soil water content data is available at 1-km resolution at three different column depths: 100, 150 and 250 cm. These levels correspond with root zone depth, reliable bedrock information and the maximum depth for which data was available, respectively. The 250 cm depth was used for this analysis. The soil database was created by a combination of soil survey maps, county and state general soil maps, and state major land resource area maps. Where no soil data were available, Landsat imagery was utilized. Each map unit may consist of as many as 21 units, with up to six layers per unit including characteristics such as percentage of map unit area, surface texture, slope range, flooding category, etc. Details of the procedure may be found in the State Soil Geographic Data Base (STATSGO) Data Users Guide [http://www.aces.edu/waterquality/data/soils/statsgo/statsgo-user-guide.pdf] (October 2006), and Miller and White (1998).

PDSI computation

Monthly precipitation for PDSI calculations was taken directly from PRISM. However, monthly mean temperature input was calculated from PRISM monthly mean maximum and minimum temperature (degrees centigrade) values. The temperature data is also used for the Thornthwaite coefficient I (Thornthwaite, 1948) calculation where I is the sum of (Equation 1) for each month and t is the mean monthly temperature:

$$\left(\frac{t}{5}\right)^{1.514} \tag{1}$$

The second Thornthwaite coefficient A is a function of I and is calculated by

$$6.75\bullet10^{-7}I^3 - 7.71\bullet10^{-5}I^2 + 1.79\bullet10^{-2}I + .49 \tag{2}$$

The next input for the PDSI is the negative tangent of the latitude. The latitude and longitude data were provided for each of the four corners in the PRISM metadata as well as the interval between grid points. Finding latitude was a simple calculation of the number of grid points from the corner multiplied by the interval.

Diaz (1983) describes a PDSI drought event as three or more consecutive months with a value of ≤ -2, ending the drought event the last month the PDSI value was at that value. The commonly used PDSI threshold value of ± 2 is used for most of the analyses discussed in this paper.

Standardized precipitation index (SPI)

The main motivation behind using the SPI for this analysis was its simplicity and temporal flexibility over other indices. SPI requires only precipitation as its input, and can be tailored to short-term timescales for agricultural drought, or long-term timescales for groundwater and reservoir supplies. The SPI is a relatively new index developed by McKee *et al*. (1993, 1995) to give a better representation of anomalous wet and dry compared to PDSI.

The SPI is a probability-based indicator of drought in that it is essentially a standardized transform of the probability of the observed precipitation (Guttman, 1999), or a statistical z-score representing the precipitation deficit over a specific time scale relative to the climatology (Steinemann, 2003). Standardizing the precipitation allows the index to be used as a comparison of drought severity across different hydrologic regimes (Bordi and Sutera, 2004). The temporal versatility is important because it allows the user to monitor the development and decline of a drought, which has been difficult to track with other indices (Hayes *et al*., 1999). However, because of its computation being closely related to the normal distribution, severe and extreme droughts occur with nearly the same frequency; therefore, it cannot be used to identify more drought-prone regions (Hayes *et al*., 1999).

The adjective classification of the index values provided by McKee *et al*., (1993) is given in Table II. Though several different index values were examined in this study, ± 1 is the primary index value discussed here, based upon McKee *et al*. (1993) and Bordi *et al*., (2001).

There are many advantages to using the SPI. Guttman (1997) suggests its use because of its simplicity, requiring only precipitation as an input. The SPI is spatially invariant in its interpretation and probabilistic so that it can be used in risk and decision analysis. It is very flexible in varying timescales from monthly to seasonal to multiyear.

However, there are also some issues to consider. SPI has varying probability differentials for equal index differentials, meaning the probability of change from -1 to -1.5 is not the same as that from -2 to -2.5 (Steinemann, 2003). Another issue with the SPI is its inability to define a drought in areas of extremely low precipitation at small timescales. The results of the present study frequently showed areas in southern California and the Southwest, where zero or near zero number of droughts occurred for the entire time period using the 1- and sometimes 3-month SPI. This was due to the fact that the median precipitation for these areas, for the period of record, was zero. When the timescales

Table II. SPI index values and adjective classifications.

Value	Class
≥ 2.00	Extremely wet
1.50 to 1.99	Very wet
1.00 to 1.49	Moderately wet
$-.99$ to .99	Near normal
-1.00 to -1.49	Moderate drought
-1.50 to -1.99	Severe drought
≤ -2.00	Extreme drought

DOI: 10.1002/joc

were increased and more months were used, this problem was resolved. Guttman (1999) concluded that, because of data limitations, timescales greater than 24 months might be unreliable. Timescales of greater than 24 months are analyzed in this study, but the points highlighted by Guttman need to be considered in the context of these longer timescale results.

Thirteen SPI indices were created for each month during the period of 1895 to 2003 including 1-, 3-, 6-, 12-, 24-, 36-, 48-, 60-, 72-, 84-, 96-, 108- and 120-month indices. The SPI indices were created using a FORTRAN 77 program available at [http://ccc.atmos.colostate.edu/standardizedprecipitation.php] (October 2006). The creation of the SPI indices was straightforward because the only input needed was the PRISM precipitation data. The first step in calculating the SPI is to determine the probability density function describing the long-term precipitation series. Next, using an incomplete gamma distribution function, the cumulative probabilities of the observed precipitation amounts are computed. Last, the inverse normal (Gaussian) function with a mean of zero and variance of one is applied to the cumulative probability (Guttman, 1999). A more extensive method of computing the SPI including formulas can be found in Guttman (1999), Bordi *et al*. (2001) and Steinemann (2003). The output from the SPI contains a monthly time series for each of the 13 indices for each grid point.

Analysis details

For the spatial and temporal analyses, a definition of an anomalous precipitation regime was necessary for each index. For the SPI, a drought event (wet event) begins when the SPI value goes below zero (above zero), decreases (increases) to at least a given threshold and then ends when the SPI goes above (below) zero again (McKee *et al*., 1993). For this analysis, 10 threshold values were chosen: -3, -2, -1.5, -1, -0.5, $+0.5$, $+1$, $+1.5$, $+2$ and $+3$.

Because of the high-spatial resolution of the PRISM data, very small areas of anomalous precipitation (less then 16 km^2) occurred. These smaller areas made the computational recognition of larger area boundaries difficult to identify. For this reason and the difficulty in quantifying these areas, a variety of filters were tested to smooth the spatial noise. A 7×7 median filter (Carr, 2002) was finally determined to give the best results (Figure 1). At the very most, this would result in the smoothing over of a 384 km^2 area.

Following the spatial smoothing, both drought and pluvial areas were identified by month for each of the 13 SPI indices and the PDSI using each of the 10 thresholds. Areas of anomalous precipitation regimes were identified by tracing the perimeter of each area including any interior holes that occurred within the shape of the areas. Sizes were computed by the number of grid cells contained inside each of the identified areas. Using Figure 1(b) as an example, four drought areas can be identified with sizes from map top to bottom of 9400, 93 400, 3400 and 58 200 km^2, respectively.

Once the size and number of areas were identified, a spatial analysis for each month was performed. This included creating a monthly time series for each index of the total area of the country that exceeded a threshold. Another analysis included using the largest drought/pluvial event for each year to observe areas with the highest frequencies of large droughts. Summary statistics for each index and threshold were also computed, including mean length of events, mean number of events, percent of time exceeding the threshold and a simple correlation of number of events and duration.

RESULTS

Spatial resolutions

When Soulé (1992) increased resolution from statewide averages to climate divisions, he stated that the statewide averages filtered out some of the mesoscale variability in drought characteristics, and noted the importance of higher spatial resolution for examining intraregion variability of drought characteristics. In this study, 4-km PRISM data provides a much more detailed look at precipitation anomalies than can be provided by using coarse data sets such as statewide averages, climate divisions, proxy reconstructions and coarse-gridded reanalysis data. For example, using 1-month SPI climate division data obtained from the Western Regional Climate Center (WRCC) and the PRISM data calculated for this project, Figure 2 shows that generally the two spatial resolutions highlight similar regions of anomalous precipitation. However, there can be substantial disagreement in the magnitude of the anomaly. An example can be seen in the climate division map (Figure 2(a)) over central Idaho and southwestern Montana in comparison to PRISM (Figure 2(b)). PRISM shows an extensive area of values less than -3, whereas the climate division values are only between -1 and -2.

While the climate division data represents the extent and intensity of anomalous precipitation for a coarser scale, it, not surprisingly, lacks the detail in higher-resolution data such as from 4-km PRISM. Because of this, some climate divisions are indicated with values that may not be contiguous throughout an entire climate division. This is often particularly problematic for larger divisions in the West with large elevation differences across a division, but can be seen elsewhere. For example, northeastern Arkansas (Figure 2(a)) has a value between -1 and -2 for the climate divisions; however, the PRISM (Figure 2(b)) shows only part of the areas covered by climate divisions as having values of -1 to -2, while the rest have values of 0 to -1.

These differences may only be relevant in certain situations such as model validation and local planning. But if a significant number of these differences occur in a single area, this could easily lead to overstatements of a particular anomaly. An example of this can be seen in the state of Kentucky. On the climate division map (Figure 2(a)), the 1-month SPI values in Kentucky appear to be almost

DOI: 10.1002/joc

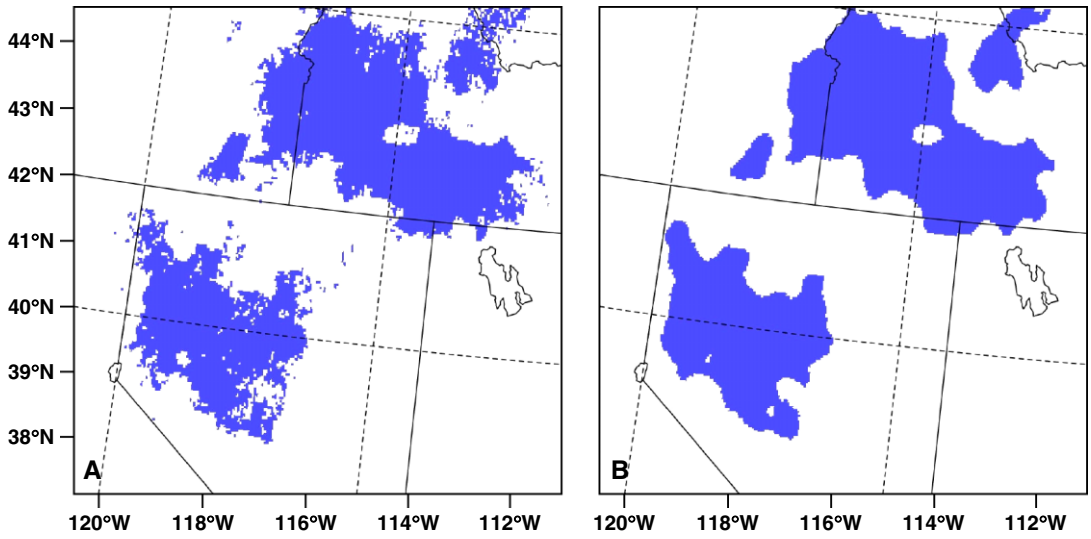

Figure 1. Example of the 7 × 7 median spatial filter smoothing used on the 4-km SPI and PDSI values showing (A) before filter and (B) after filter. This figure is available in colour online at www.interscience.wiley.com/ijoc

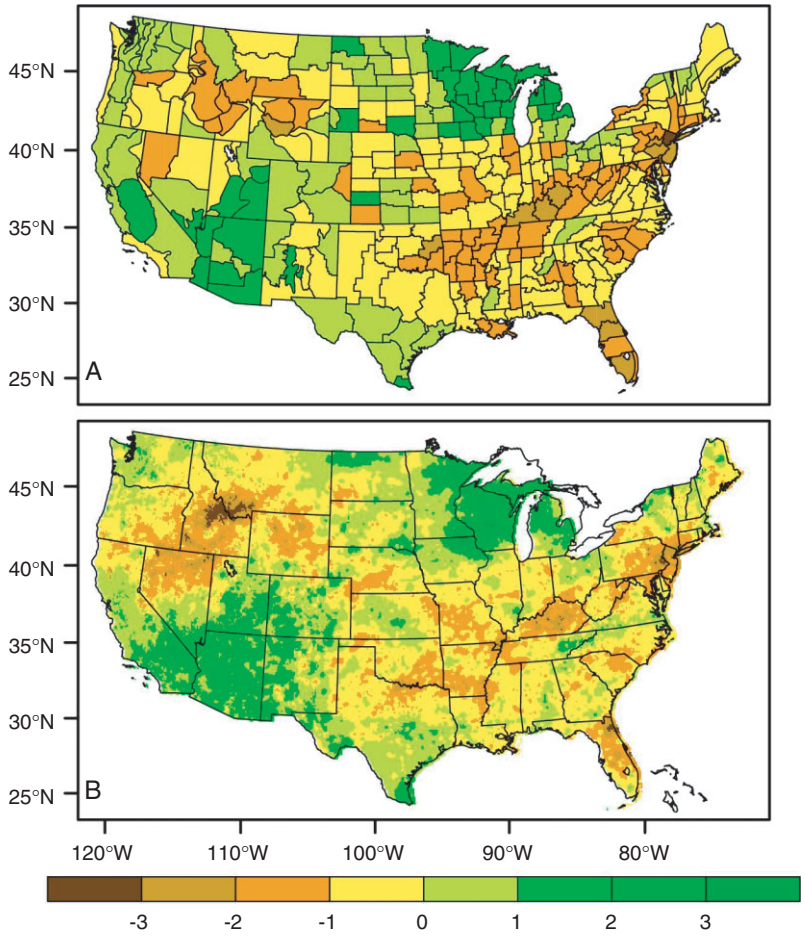

Figure 2. 1-month SPI for July 1999 showing (A) index values based on climate divisions and (B) index values based on PRISM data. Color scale denotes SPI index value. SPI threshold definition is −1.

entirely in the range of −3 to −2, whereas the PRISM map shows only a scattered area with such values. The rest of the state had values ranging from 0 to −1.

The box plots in Figure 3 show 1-month SPI value distributions for four sample climate divisions using PRISM data. Each respective climate division value is indicated by a square symbol. The southern climate division of the central valley of California was chosen because of its large size and apparent difference in values between the two maps in Figure 2. The easternmost

DOI: 10.1002/joc

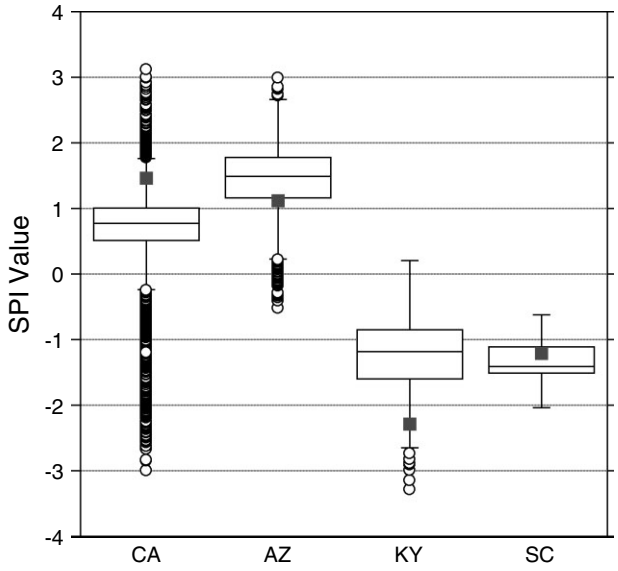

Figure 3. Box plots of 1-month SPI values from PRISM data within four selected climate divisions. Box symbol denotes original climate division value.

climate division in Kentucky was also chosen because of the differences in values between the two maps. Two more climate divisions, the southernmost climate division in Arizona and the northcentral climate division in South Carolina, were chosen to represent areas where the two maps appeared to agree.

The climate division values for California and Kentucky clearly are well outside the middle 50% range. In the Kentucky case, the individual PRISM would suggest a wetter division value than what is depicted by the actual climate division value. The California case suggests that the division is much drier than indicated by the actual climate division value. This case is also particularly interesting because it is a large western division, and consequently shows a large range of PRISM values basically from -3 to $+3$.

The Arizona and South Carolina climate divisions were chosen because the SPI values from the PRISM and climate divisions appeared similar on the map. For the South Carolina case, the actual climate division value and the PRISM distribution appear to correspond reasonably well. However, in the Arizona case, the actual climate division values fall just below the PRISM's 25th percentile value, and there is a fairly large range of PRISM values including several outliers. These four examples raise interesting questions on not just how well PRISM agrees with climate division values but also on the appropriate size and geographic representation of climate divisions.

Brief comparison of SPI and PDSI

The PDSI has an inherent timescale of 6 to 12 months (Redmond, 2002). Comparing PDSI values with the 6- and 12-month SPI provides an indication of how the two index methods are associated in a high-spatial resolution setting. Figure 4 shows an example of the PDSI (Figure 4(a)), the 6-month SPI (Figure 4(b)) and 12-month SPI (Figure 4(c)) for February 1898. Overall, the three indices match well. For example, all indices show southern Utah in drought conditions, while Georgia and South Carolina are abnormally wet. However, the areas do differ in the size and intensity of extremes. In

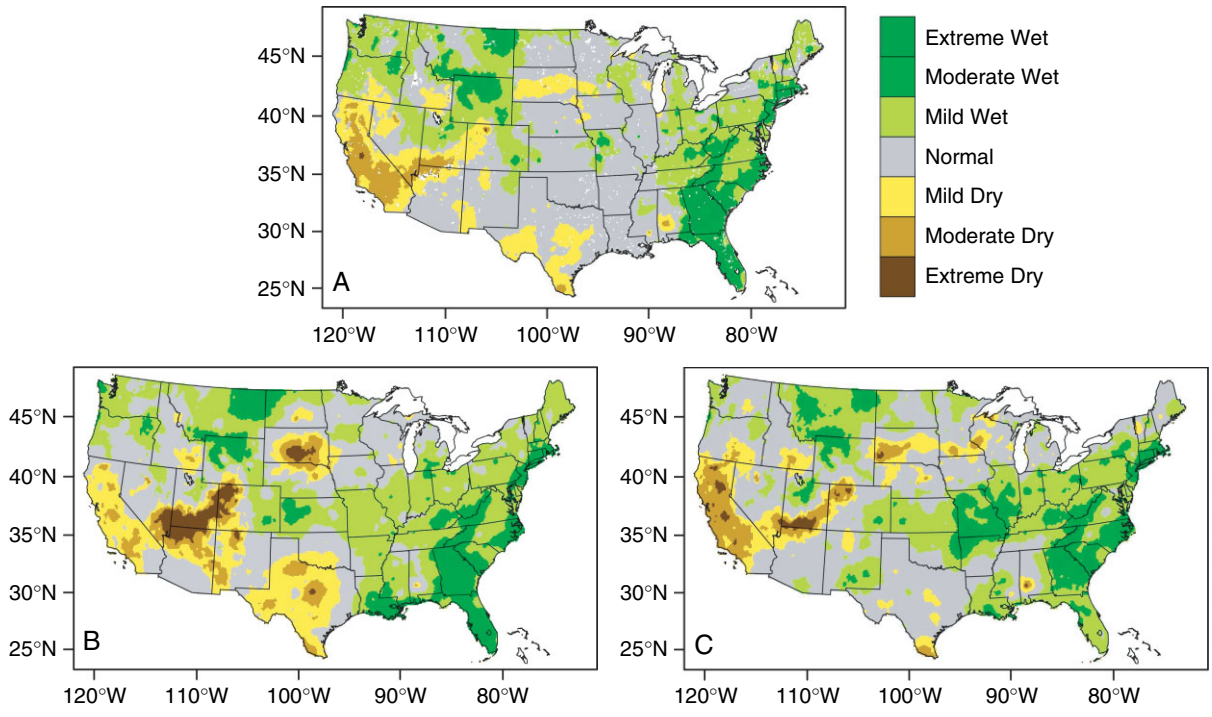

Figure 4. Maps comparing February 1898 index values for related timescales for (A) PDSI, (B) 6-month SPI and (C) 12-month SPI. Color scale denotes index classification.

DOI: 10.1002/joc

some cases, the same location may be abnormally dry for one index and wet for another. For example, most of western Kansas has mild drought values given the PDSI, but mildly wet values given the 6-month SPI. In another example, southern Utah SPI values indicate an extreme drought, while PDSI values show only a moderate drought.

In some cases, the PDSI may more closely resemble the 6-month SPI results, while in other cases the 12-month SPI. For example, the PDSI and the 12-month SPI show a similar moderate drought in California that is not as extensive or severe in the 6-month SPI. The opposite occurs in the southeast where the PDSI and 6-month SPI cover similar areas but the 12-month SPI values differ. This does not imply that the 12-month SPI and PDSI always correspond for drought and the 6-month SPI and PDSI correspond for wet periods, but instead they are both variable over time and space. Ultimately, the choice of index usage is dependent upon user or practitioner needs based upon experience and other factors. Ideally, it would be desirable to allow for comparison of indices for many applications. We do not make a recommendation of one index over another, and here simply offer a simple example of how differences may appear within a high-resolution dataset. Clearly, more detailed analysis would be required to assess consistent similarities or differences between the indices.

Total monthly drought area

Figure 5 represents the total area and percentage of the country under drought (≤ -1 SPI; ≤ -2 PDSI) for each month of the study period for eight different indices, including seven SPI timescales and the PDSI. The short timescales, such as the 1-, 3- and 6-month SPI, show substantial intraseasonal variability. As the timescales of the indices become longer, the more lengthy droughts begin to stand out as would be expected. Substantial interannual variability is seen at the longer time scales. Longer timescales have a lag until a threshold event occurs; because of this, it is possible to be under drought conditions during one timescale and under normal or abnormal wet conditions in another. Particularly evident in the 72-month SPI is a decrease in US drought area starting around 1970.

The statistics in Table III were computed from the data used to make the time series seen in Figure 5. The mean and standard deviations of the area were calculated along with the sizes of the largest and smallest drought areas. Mean values are quite similar for each of the timescales, but increase slightly by about 60 000 km^2 from the 1-month to the 72-month SPI. The PDSI has the smallest mean area compared to the SPI indices. Variance increases with timescale as shown by standard deviation values increasing by 150 000 km^2 from the 1- to the 72-month SPI. The maximum drought area sizes occur on the shorter timescales; from the 1- to the 72-month SPI, there is almost a two million square kilometer decrease in the maximum size. Conversely, the minimum drought area sizes are quite variable and show no trend with size.

Table III. Descriptive summary statistics for each of the drought time series shown in Figure 4. Statistics include the mean, standard deviation, maximum and minimum. Units are US area in thousand square kilometers.

Index	Mean	S.D.	Max	Min
1 month	1157.6	768.5	6238.7	10.4
3 month	1190.1	763.8	4684.4	6.0
6 month	1211.5	815.8	5416.6	26.3
PDSI	1050.5	763.8	4214.5	34.2
12 month	1209.9	856.8	4747.2	51.1
24 month	1234.1	909.8	4363.2	11.3
36 month	1224.8	904.3	3971.4	12.6
72 month	1217.8	905.4	4259.3	16.9

Total monthly pluvial areas

Figure 6 shows the total pluvial area ($\geq +1$ SPI; $\geq +2$ PDSI). In many respects, pluvial results are similar to those for drought. The short-term indices exhibit substantial intraseasonal variability with some months approaching nearly 50% of the country undergoing pluvial conditions. The 72-month SPI indicates a change toward a more dominant wet regime starting around 1970, following at least a 70-year period of dominant dry.

Table IV summarizes the descriptive statistics for the pluvial time series (Figure 6). The mean pluvial areas for all of the indices are very similar, with the exception of PDSI that has the smallest mean value. The variance increases at the longer timescales as there is almost a 400 000 km^2 standard deviation increase from the 1- to the 72-month SPI. Neither the maximum nor the minimum values for the pluvial data show any obvious patterns given the timescale, except that the minimums are over twice as large for the longest timescales (i.e., 36- and 72-months).

The number of studies of pluvial events is fewer than those for drought. Fye *et al*. (2003) discuss one large pluvial that overlaps the study period in this paper. Using regionally averaged summer PDSI values, Fye *et al*. (2003) reported that from 1905 to 1917 much of the West was in a period of anomalous wet. However, using the PRISM data, the years 1905 to 1917 do not stand out given any of the indices in comparison to other later periods, though the 12-, 24- and 36-month SPI indices

Table IV. Same as Table III except for pluvial time series in Figure 5.

Index	Mean	S.D.	Max	Min
1 month	1183.7	677.3	4403.6	22.7
3 month	1200.1	737.4	4824.3	11.0
6 month	1211.7	757.0	4217.3	24.7
PDSI	969.8	682.4	4192.6	3.7
12 month	1214.3	813.5	4069.8	13.2
24 month	1213.3	906.3	4240.2	34.8
36 month	1214.1	949.8	4297.2	58.9
72 month	1241.2	1054.2	4929.1	47.9

DOI: 10.1002/joc

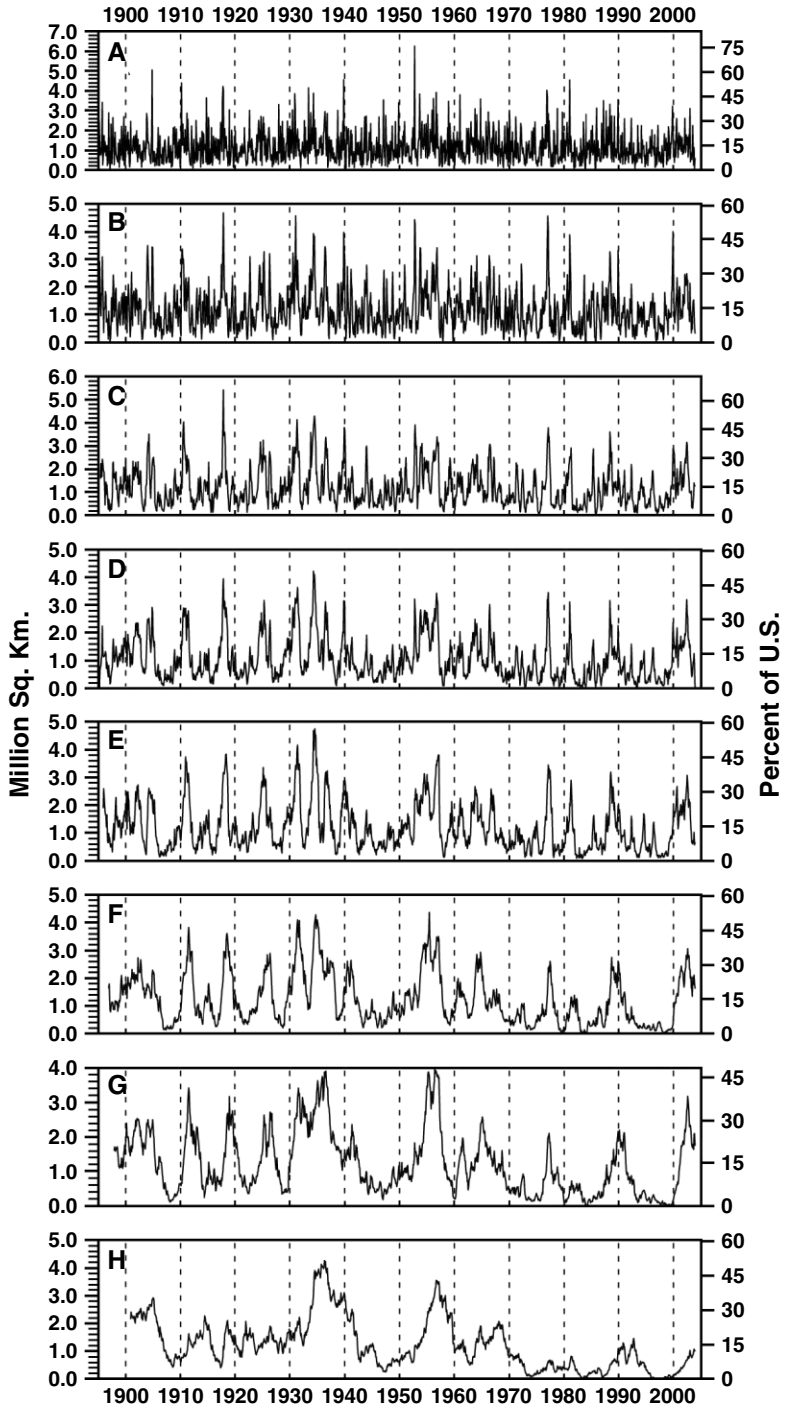

Figure 5. Monthly time series plots representing the total drought area (in million square kilometers) for eight drought indices with the corresponding percentage of area given on the right axis for (A) 1-month SPI, (B) 3-month SPI, (C) 6-month SPI, (D) PDSI, (E) 12-month SPI, (F) 24-month SPI, (G) 36-month SPI and (H) 72-month SPI. Note that different scales are used as needed to highlight individual plot features rather than a direct comparison of the indices.

do show pronounced peaks. The years 1905 to 1917 do not appear to be one continuous pluvial, but instead two smaller pluvials centered around 1905 and 1917 with a drier period in between.

The Fye *et al*. (2003) paper claims that the period of 1905–1917 was the largest and longest pluvial of the 20th century. However, the results from the present analysis suggest a different conclusion. For example, a much larger portion of the country had anomalous wet conditions around 1942, and, for indices of 24 months or greater, this wet period lasted for a decade or longer until the drought of the 1950s. But perhaps even more apparent is the most recent 30-year period showing three pluvials, all of which are larger and longer lasting than any other in the record. Post-1970 overall has larger percentages of pluvial area and higher frequency of events compared to pre-1970 as indicated by all of the indices with the exception of the 1-month SPI. This is in agreement with

DOI: 10.1002/joc

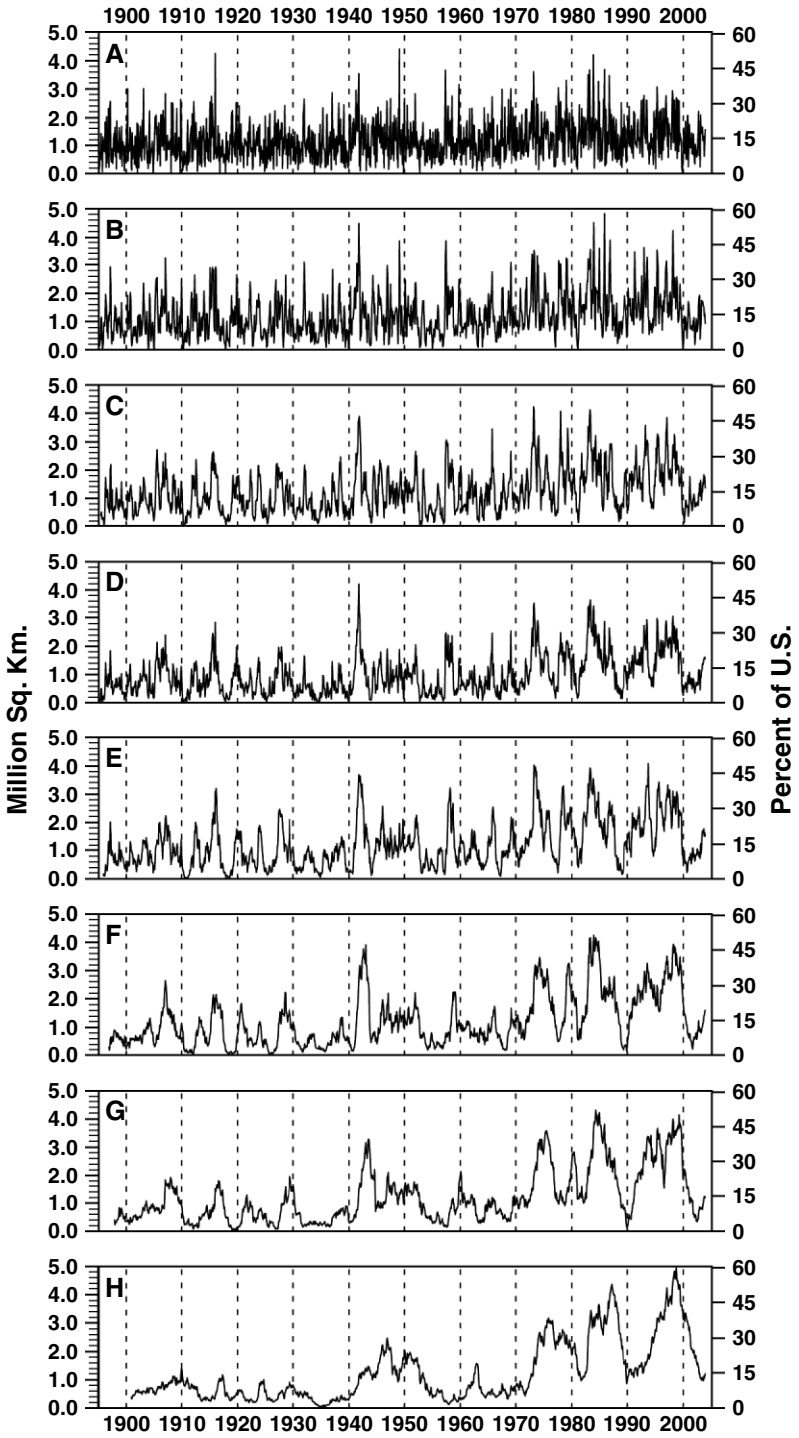

Figure 6. Same as Figure 5 except for pluvial.

the Karl *et al*. (1996) study showing that there has been an increase in anomalous wet events since 1970. The decline in the most recent wet period also corresponds with the beginning of a dry period in 2000; a notable multiyear drought in the West began in 1999.

The difference in conclusions between this analysis and that of Fye *et al*. (2003) is likely a result largely from the use of regionally averaged summer PDSI values and the use of different datasets. The high-resolution PRISM data clearly provides more detail compared to the 1036 single station monthly PDSI records from the Historical Climatology Network and tree ring reconstructions used by Fye *et al*. (2003). While using regionally averaged summer PDSI values may have been the best way to correlate instrumental data with tree ring chronologies, it missed a major portion of the annual precipitation budget. This is especially true in the West in which most of the moisture recharge is from winter snowfall/snow pack. While the larger pluvials seen in this study may have been partly due to the increased resolution, it was

DOI: 10.1002/joc

certainly the addition of the entire year's precipitation budget that made the biggest difference. The summers of 1905 to 1917 may be some of the wettest on record, but it is the annual values since 1970 that have been the wettest based on PRISM.

Closer look at pluvial events

Figures 7 and 8 offer a closer look at the extreme annual wet periods for the three decades following 1970. The maps show the 1905–1917 period discussed in Fye *et al.* (2003), as well as three separate periods chosen on the basis of the three distinct peaks in the 72-month SPI (Figure 6(h)); 1973–1981, 1983–1988 and 1990–2000. Two indices were chosen: the 12-month SPI (Figure 7) to represent shorter scale pluvials and to represent a similar timescale as the PDSI, which was used by Fye *et al.* (2003) and the 72-month SPI (Figure 8) to represent long-term pluvials. The scale represents the number of years out of the given period total (i.e., 13, 9, 6 and 11 years, respectively) that the largest pluvial occurred for each PRISM grid cell.

Figure 7(A) shows the spatial extent of the 1905–1917 pluvial that is larger here than described in the Fye *et al.* (2003) paper. Not only was most of the West under a period of anomalous wet but also a large portion of the East. Figure 7(B) shows a 1973–1981 pluvial period of which the area is distributed over a larger portion of the country compared to the 1905–1917 pluvial, although it is only in the southeast where the most number of wet years occurred (6 out of the 9 years were anomalous wet during this period). The pluvials of 1983–1988 and 1990–2000 (Figure 7(c) and (d)) also extend over a larger portion of the country compared to the 1905–1917 events. The 1983–1988 pluvial (Figure 7(c)) has a larger area compared to 1905–1917, especially in the West. The 1990–2000 pluvial (Figure 7(d)) is clearly the largest including almost the entire country. These maps indicate that the pluvial of 1905–1917 was widespread, but was at least equaled or exceeded spatially by three periods since 1970 in this dataset.

Figure 8 shows the 72-month SPI for the same periods to indicate longer-term anomalous wet. The 1905–1917 pluvial (Figure 8(a)) no longer covers an area as extensive as in Figure 7(a). This shows that while the pluvial may have been extensive in terms of short timescales, it was not as extensive at the longer time scales. However, while the 1970s pluvial (Figure 8(b)) covered a large portion of the country in the 12-month SPI (Figure 7(b)), this pluvial was concentrated on the East coast over the longer time scale. The pluvial of the 1980s (Figure 8(c)) has similar characteristics to the 12-month SPI (Figure 7(c)), but is most notable in the West. The 1990s pluvial (Figure 8(d)) is widespread similar to the 12-month SPI (Figure 7(d)), but is very much dominated by the large number of wet years in parts of the southcentral region.

Largest annual areas of precipitation anomalies

Since the SPI is a standardized index, all areas of the country are equally as likely to experience drought or pluvial, and all areas should experience the same number of wet and dry events over the long term.

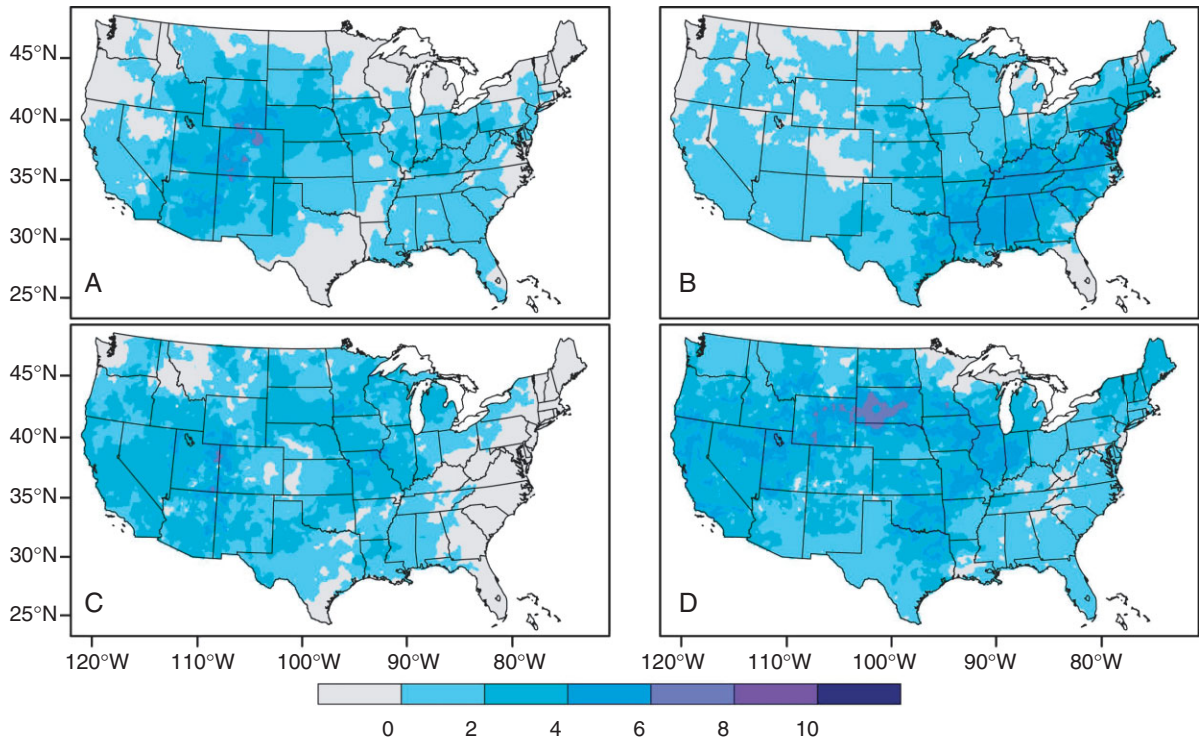

Figure 7. Maps showing number of years of occurrence out of the period total for the largest annual pluvials based on the 12-month SPI for (A) 1905–1917, (B) 1973–1981, (C) 1983–1988 and (D) 1990–2000. Color scale indicates the number of years. Threshold definitions are −1 for SPI and −2 for PDSI.

DOI: 10.1002/joc

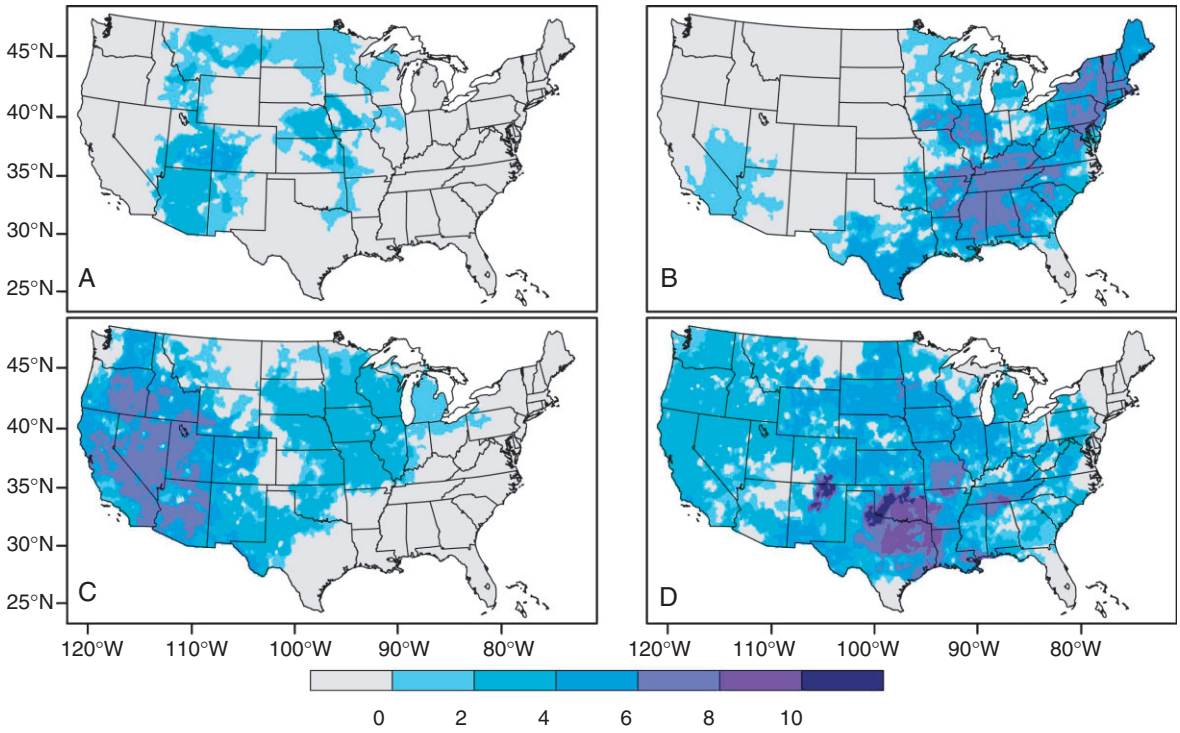

Figure 8. Same as Figure 7 except for 72-month SPI.

Therefore, simply looking at the total number of droughts for the country or the percent of time in drought or pluvial reveals almost homogeneous values for the entire United States. In order to examine drought and pluvial spatial patterns, the largest annual areas of precipitation anomalies for the period of record were compiled. A composite of each year's largest annual anomaly area yields a total count (out of a possible 108 years) of how often each grid cell over the United States has been associated with the largest drought and pluvial contiguous areas. The thresholds of ± 1 for the SPI and ± 2 for the PDSI are used in this analysis.

Figure 9 shows the results of the largest drought areas for the PDSI and seven SPI indices. The 1- and 3-month SPI indices (Figure 9(a) and (b)) agree with previous studies showing drought occurrence less dominant on the coasts and more dominant in interior United States. (Soulé, 1992). The states in central United States have the highest values with counts of over 40 and 50 years or greater than 40 to 50% of the time, gradually decreasing in occurrence toward the coasts. The Pacific Northwest, Florida and Maine have the lowest occurrences of drought in the 1-month SPI (Figure 9(a) and (b)) with events occurring less than 10 years within the 108-year period. The remainder of the country for the 1- and 3-month SPI has counts of between 10 and 30 years. These counts indicate that 1- and 3-month droughts occur throughout most of the country around 25% of the time.

The PDSI map (Figure 9(d)) differs from the 6- and 12-month SPI (Figure 9(c) and (e)), though it more closely matches the 12-month map. Higher counts occur in the Southwest with the PDSI than with the 12-month SPI. However, the 6-month SPI has a much larger area of 20–30 year counts than does the PDSI.

Over longer timescales, most of the country becomes more homogeneous in drought area occurrence with a few persistent patterns. Florida and Maine have counts of 10 or less years for all of the indices, and the central and western United States has counts upward of 40 years but decreasing at the longer timescales. Obviously, the number of events decreases with the longer timescales because of a shorter available record. The 12- and 24- month SPI maps have counts of up to 30 years, but the 72-month SPI remains below 20 years.

The largest annual areas for pluvial events were constructed in the same manner as the drought events and are shown in Figure 10. Similar to the drought maps in Figure 9, the largest pluvial events are more prevalent in the interior of the country, and less prevalent on the coasts for the 1- and 3-month SPI (Figure 10(a) and (b)). However, while the highest drought occurrence is centered on southern Missouri for the 1-month SPI, the highest pluvial is centered in eastern Kansas for the same index (Figure 10(a)), and is smaller in area for the maximum occurrence (40–50 years). The drought counts for the 1- and 3-month indices are slightly higher than the pluvial counts for the same indices by approximately 10 years (55 and 45 years, respectively). The PDSI pluvial map (Figure 10(d)) appears generally similar to the 12-month SPI, but compared to the drought PDSI map (Figure 9(d)), the maximum areas of occurrence are shifted north to the central and northern plains region, and reduced in the western region.

DOI: 10.1002/joc

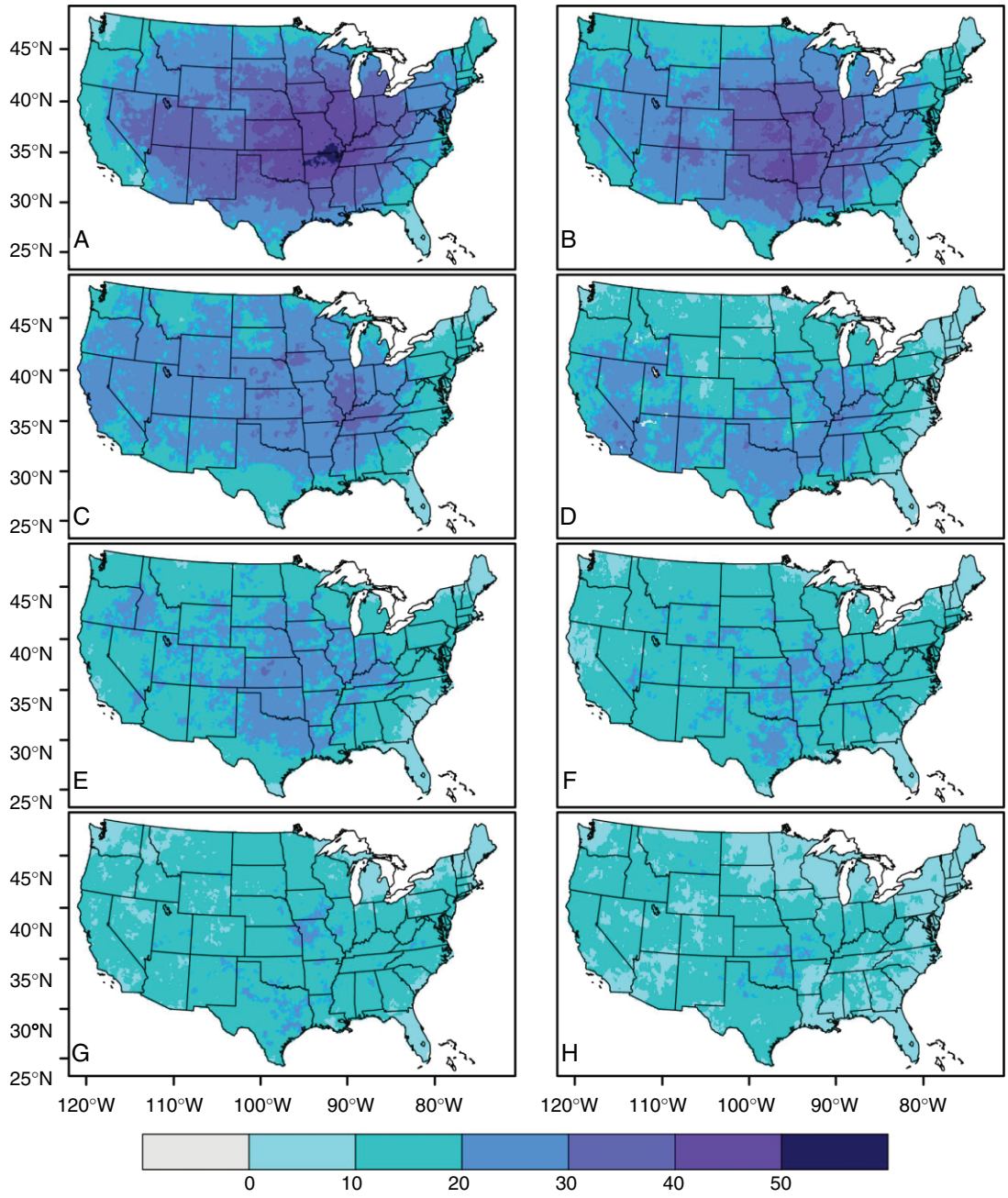

Figure 9. Maps of largest annual drought area occurrence for (A) 1-month SPI, (B) 3-month SPI, (C) 6-month SPI, (D) PDSI, (E) 12-month SPI, (F) 24-month SPI, (G) 36-month SPI and (H) 72-month SPI. Threshold definitions are −1 for SPI and −2 for PDSI. Color scale represents the number of years a drought occurred during the 1895–2003 period.

Diaz (1983) found that areas more prone to drought, such as the central United States, are also more prone to periods of anomalous wet. The results in this study confirm that the largest areas of positive and negative anomalous precipitation appear in basically the same geographic locations (especially for the 1- and 3-month SPI indices), and that the areas of most frequently occurring drought or pluvial events are in the central United States.

Figure 11 shows the association between area (in thousand square kilometers) and index by taking the largest annual drought/pluvial areas for each index and averaging them over the period of record. The graph shows that the average size of the largest annual drought area decreases with the longer timescales (solid curve). For example, the average size of the largest annual drought area (approximately 126 000 km^2 for 1-month SPI) decreases by more than 50% to 62 000 km^2 for the 36-month SPI. Pluvial areas (dashed line) show a similar relationship to the index timescale.

The annual largest areas of precipitation anomalies occurred with a higher frequency during the months of December and January for both positive and negative anomalies (Figure 12). The occurrence of winter season anomalies is over twice that of summer season. Karl *et al.* (1987) explain that for the central and northern interior United States, where frequencies of drought occurrence

DOI: 10.1002/joc

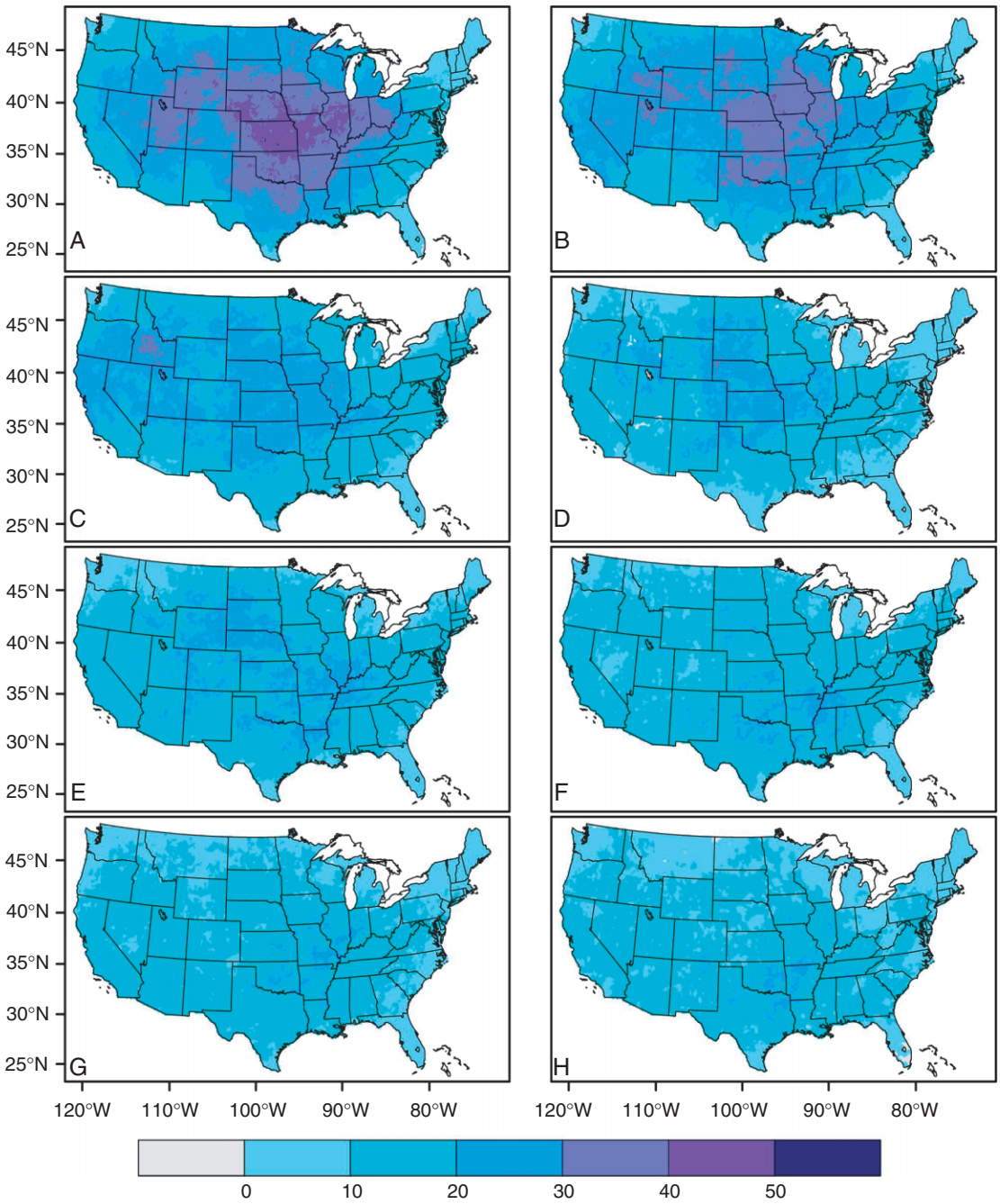

Figure 10. Same as Figure 9 except for pluvial areas and thresholds of +1 for SPI and +2 for PDSI.

are highest, there is little chance of ending an ongoing drought event during the winter months because the probability of receiving sufficient moisture for recovery is lowest. However, large positive moisture anomalies in the western United States are more likely to occur during the winter months because much of this area receives most of its annual precipitation during this season (November through March).

Changing the thresholds

Changing the thresholds for the largest annual drought areas from −1 to −2 for SPI and from −2 to −3 for PDSI (and hence highlighting more extreme conditions) reduces as expected the percent of the country covered, but does not change the geographical locations of the most frequent occurrences (Figure 13). Given an increased threshold, the highest 1-month occurrences remain east of the Rockies but are shifted eastward and centered in the Ohio River valley compared to Figure 9(a). The Pacific Northwest now stands out from the surrounding areas, though the actual occurrence has changed little. Increasing the timescales decreases the percent of the country covered. At the 24-month timescales (Figure 13(f)) and longer, there is a dominant north–south pattern running through the center of the country.

As with drought, changing the thresholds for the largest annual pluvial areas from +1 to +2 for SPI and from

DOI: 10.1002/joc

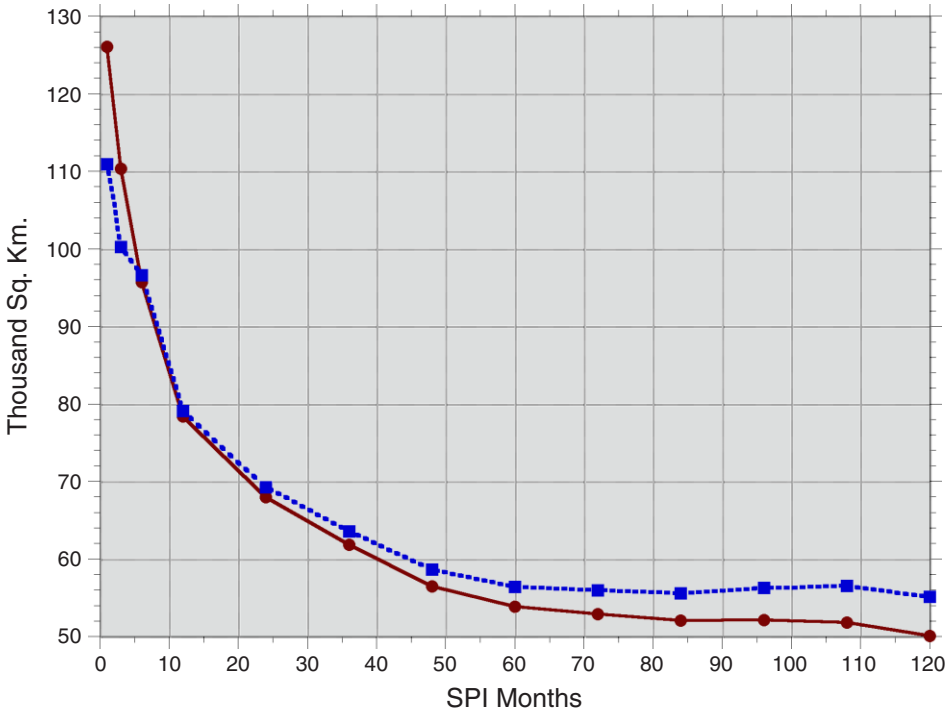

Figure 11. The average size (thousand square kilometers) of the annual largest drought (solid line) and pluvial (dashed line) area for each of the 13 SPI indices. This figure is available in colour online at www.interscience.wiley.com/ijoc

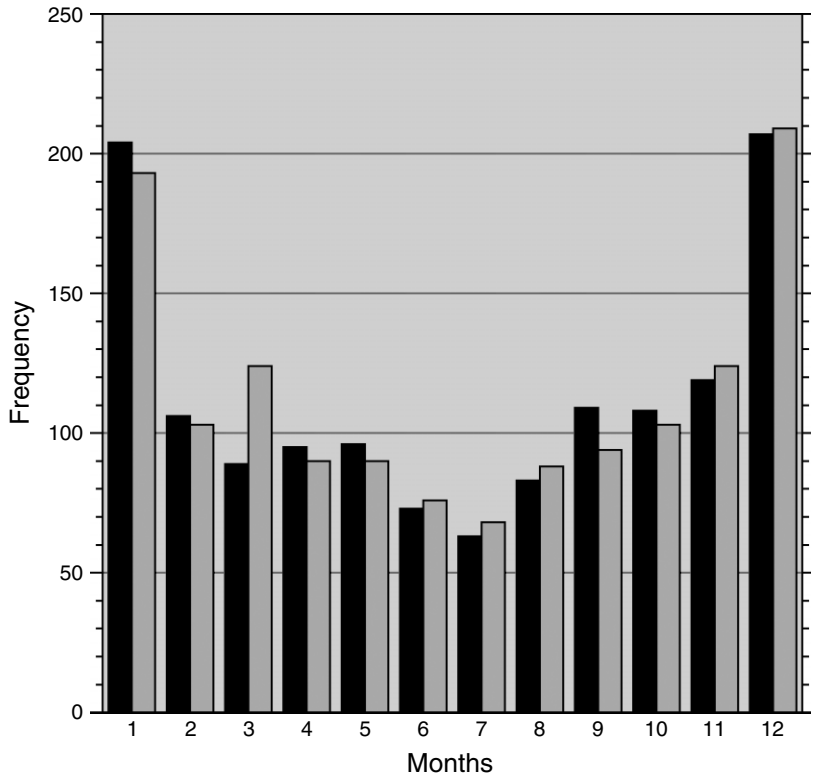

Figure 12. Frequency histogram of the monthly occurrence of the largest drought (black) and pluvial (gray) areas.

+2 to +3 for PDSI reduces as expected the percent of the country covered, and changes the locations of the most frequent occurrences (Figure 14). The 1-month occurrence area is still more or less centered in the Ohio Valley region, but is less expansive than for drought in Figure 10(a). The north–south pattern for the longer timescales does not appear in the pluvial maps. The PDSI occurrence area (Figure 14(d)) is more extensive and generally higher in occurrence than its pluvial counterpart in Figure 10(d).

DOI: 10.1002/joc

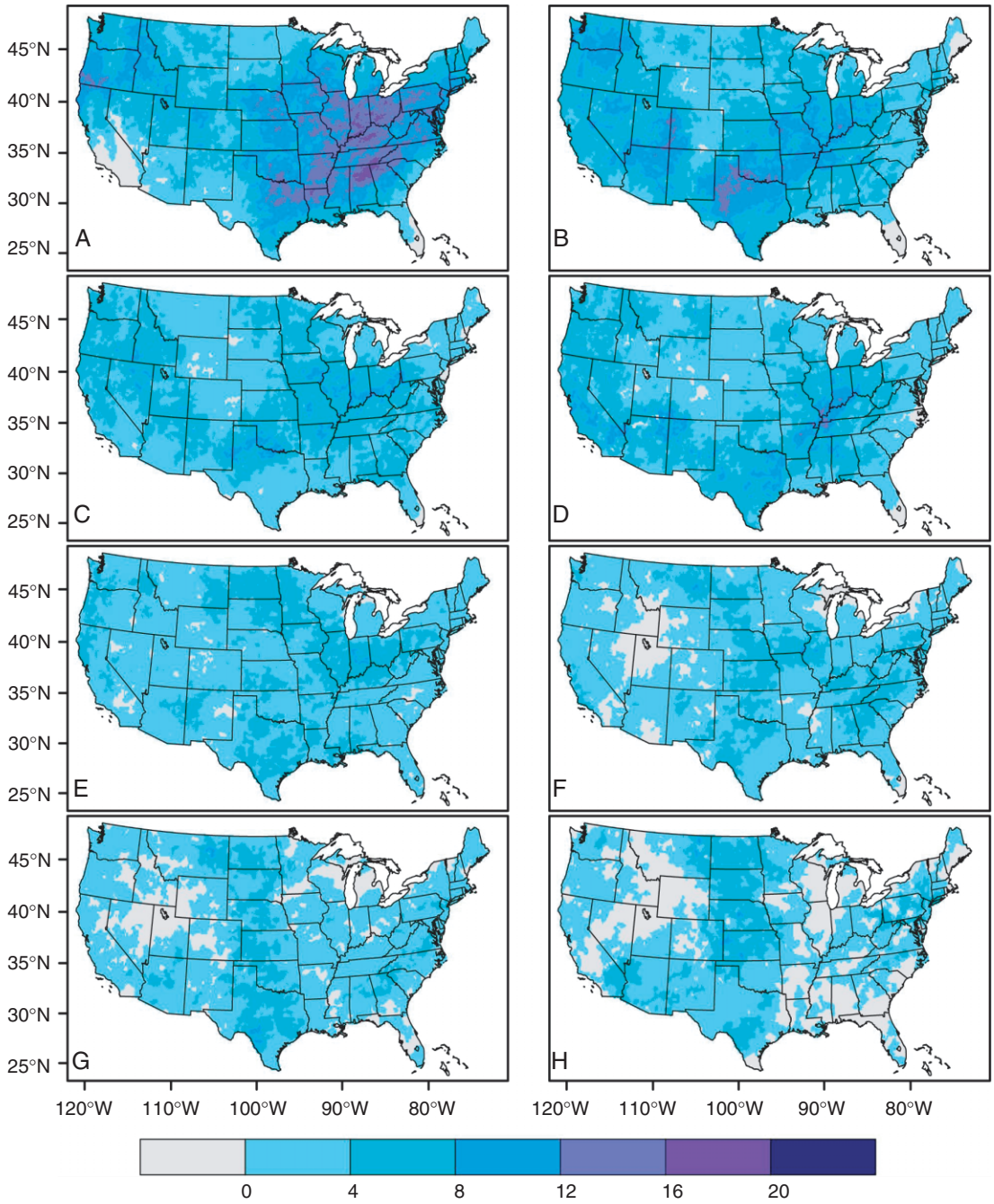

Figure 13. Same as Figure 9 except for thresholds of −2 for SPI and −3 for PDSI.

Annual extremes

The locations for the most extreme annual driest values are shown in Figure 15. While extremes are found generally throughout most of the country, there is some clustering among the various indices. The 1-month SPI (Figure 15(a)) maps show a more or less random distribution of annual extremes, but the 3- and 6-month SPI (Figure 15(b) and (c)) show most of the extremes located in the West. The 6-month SPI also has a grouping in southern California. PDSI (Figure 15(d)) also shows most of the extreme values in the West, but more clustered in the Northwest. The 12- to 72-month SPI maps show most of the extreme points in the western and the eastern portions of the country, with only a few extremes in the central region.

Figure 16 shows the locations for the most extreme wet values. The 1-, 3- and 6-month SPI and the PDSI all have the same pattern of a greater occurrence of extreme values in the West. Both wettest and driest extremes have this pattern for most of the timescales; however, it is interesting that this does not correspond to the location of the largest drought area centered in the central United States. The 12-month SPI has points in the eastern and western United States with very few in the central portion of the country. The 24-, 36- and 72-month SPI maps show a fairly random distribution of dry extremes across the country.

DOI: 10.1002/joc

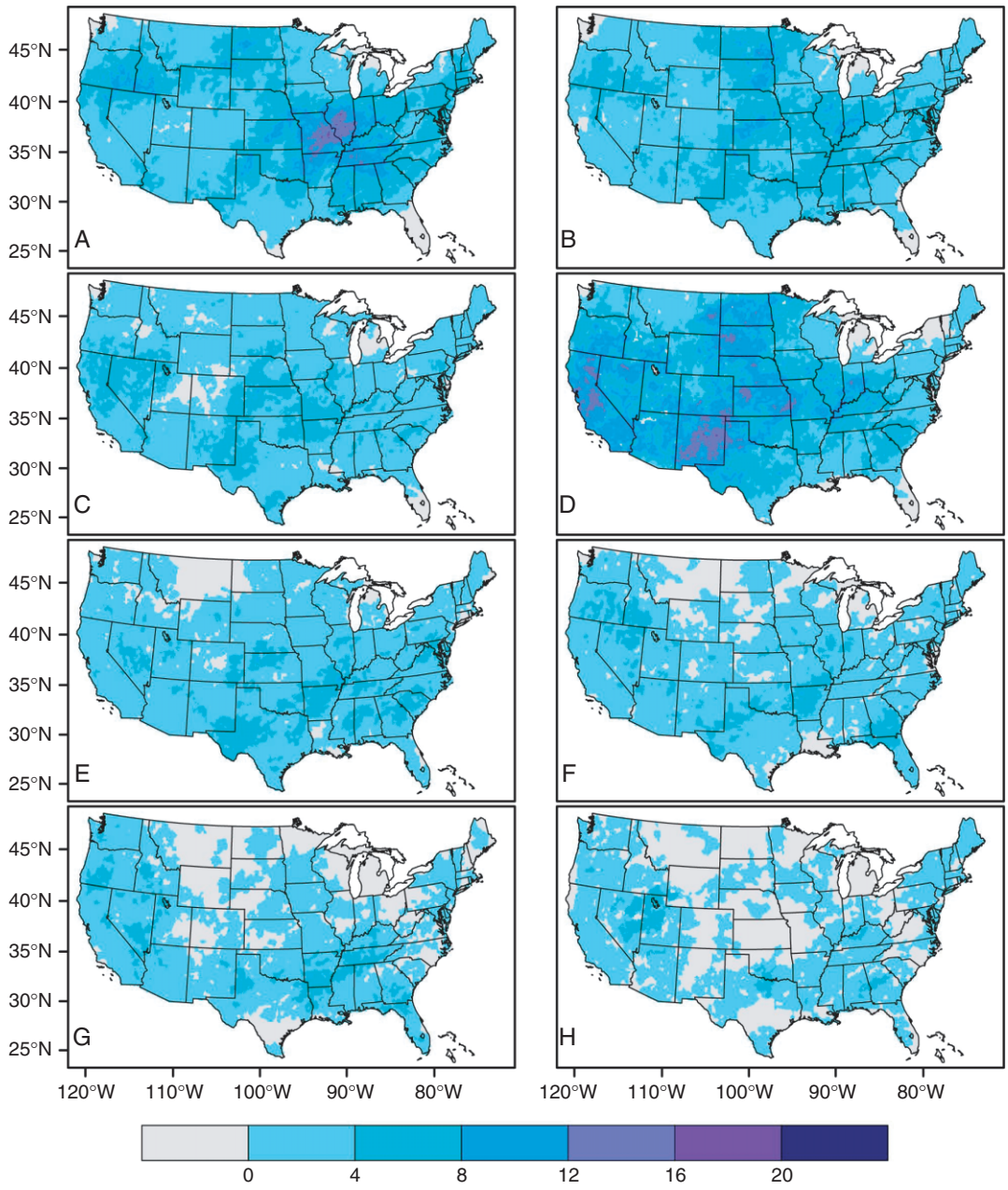

Figure 14. Same as Figure 9 except for pluvial areas and thresholds of +2 for SPI and +3 for PDSI.

Since many of the most extreme values are located in the West and often following along the Rockies, the elevations of the extremes were accumulated in histogram bins to assess possible elevation differences. Figure 17 shows the elevations of all the drought and pluvial extremes sorted into 305-m (1000-ft) bins and plotted alongside the elevations of every point in the analysis for comparison. The total numbers were then calculated as a percent. At elevations greater then 1830 m, there is an increase in the number of extremes above this height compared to the national average. This may be due to PRISM data issues at high elevations where good observed precipitation data is minimal. On the other hand, it may be that the West is more climatically susceptible to precipitation extremes due to long-wave circulation patterns and/or elevation influence.

Drought and pluvial characteristics

Some basic attributes of anomalous precipitation based on the high-resolution dataset using various timescales and thresholds for definitions of anomalous precipitation are summarized in Table V. This table is an expansion of the one provided by Soulé (1992) that presented results on drought characteristics using Palmer indices. The mean total number of anomalous precipitation events is the average number of events for every PRISM grid point in the United States. The mean length of anomalous precipitation events was calculated first by averaging the length of all events for a grid point, and then calculating the average of all grid points for the entire United States. The percentage of time spent in an anomalous precipitation event was calculated on the basis of the

DOI: 10.1002/joc

Table V. Descriptive summary statistics for each index and 10 thresholds. Column headings indicate the SPI or PDSI index. Row labels include the mean number of occurrences, the mean length of occurrence (in months), the percent of time each threshold occurs and the Pearson correlation of the number of occurrences and the length of each occurrence for each grid cell.

Index	1	3	6	12	24	36	48	60	72	84	96	108	120	PDSI
Threshold = −0.5														
Mean #	177.9	110.4	69.0	37.7	21.0	14.9	11.6	9.5	8.0	7.0	6.4	5.6	5.1	60.9
Mean length	3.1	5.3	8.5	15.5	27.3	38.7	50.2	62.4	75.5	88.2	98.7	113.1	125.9	9.6
% of time	42.3	44.7	44.9	44.8	44.4	44.3	44.2	44.2	44.3	44.2	44.2	44.3	44.4	40.0
Correlation	−0.29	−0.85	−0.89	−0.88	−0.89	−0.87	−0.86	−0.84	−0.81	−0.81	−0.79	−0.79	−0.78	−0.56
Threshold = −1.0														
Mean #	125.0	77.2	47.1	24.4	13.0	9.2	6.9	5.6	4.7	4.1	3.7	3.3	3.1	46.9
Mean length	3.3	6.1	10.4	20.1	37.4	53.4	70.6	89.9	110.2	128.2	143.6	161	177.5	8.8
% of time	31.4	35.9	37.3	37.6	37.5	37.6	37.3	37.2	37.3	37.3	37.4	37.8	38.2	28.0
Correlation	−0.31	−0.76	−0.82	−0.81	−0.82	−0.80	−0.79	−0.76	−0.76	−0.76	−0.77	−0.76	−0.77	−0.17
Threshold = −1.5														
Mean #	68.5	44.4	27.6	14.3	7.7	5.4	4.1	3.3	2.8	2.5	2.3	2.1	1.9	34.2
Mean length	3.5	7.1	12.3	24.5	46.6	67.5	91	116.3	139.6	159.3	175.7	192.8	211.5	7.7
% of time	18.3	24.0	25.9	26.8	27.4	27.7	27.4	27.4	27.4	27.7	28.4	29.0	29.9	17.7
Correlation	−0.28	−0.58	−0.74	−0.72	−0.70	−0.66	−0.67	−0.68	−0.67	−0.67	−0.67	−0.66	−0.67	−0.02
Threshold = −2.0														
Mean #	29.4	20.3	12.9	6.9	3.8	2.6	2.1	1.8	1.6	1.4	1.4	1.3	1.3	21.6
Mean length	3.7	7.9	14.3	29.0	56.9	83.8	109.4	131.6	149.7	167.2	181.5	197	216.1	6.8
% of time	8.2	12.3	13.9	15.1	15.8	16.0	16.3	16.9	17.3	18.0	18.9	19.8	21.5	9.7
Correlation	−0.09	−0.31	−0.53	−0.53	−0.52	−0.51	−0.51	−0.47	−0.41	−0.38	−0.39	−0.36	−0.36	−0.04
Threshold = −3.0														
Mean #	3.7	2.5	1.7	1.3	1.1	1.1	1.0	1.0	1.0	1.0	1.0	1.0	1.0	5.2
Mean length	3.8	8.7	15.9	32.1	65.8	84.7	102.0	114.8	125.5	138.9	154.0	155.0	158.6	5.5
% of time	1.1	1.6	2.1	3.3	5.5	7.1	8.6	9.5	10.3	11.4	12.8	13.0	13.4	1.9
Correlation	0.03	−0.07	−0.04	−0.04	−0.05	−0.08	−0.05	−0.06	−0.03	−0.02	−0.04	−0.09	−0.08	−0.05
Threshold = +0.5														
Mean #	184.1	112	68.3	36.9	20.8	14.6	11.2	9.2	7.9	6.9	6.4	5.7	5.1	44.1
Mean length	3.3	5.2	8.6	15.9	28.3	40.6	53.6	66.3	77.7	90.1	99.2	112.5	90.7	8.5
% of time	45.8	44.7	44.8	44.5	44.6	44.4	44.3	44.3	44.3	44.4	44.6	44.5	44.6	25.0
Correlation	−0.45	−0.85	−0.91	−0.90	−0.91	−0.90	−0.87	−0.84	−0.84	−0.81	−0.79	−0.79	−0.44	−0.35
Threshold = +1.0														
Mean #	127.1	73.5	44.0	23.1	12.5	8.7	6.5	5.3	4.6	4.1	3.8	3.4	3.1	35.1
Mean length	3.5	6.1	10.6	20.4	38.7	56.6	76.0	93.4	109.1	126.2	139	156.1	117.9	7.9
% of time	33.7	34.3	35.5	35.8	36.5	36.4	36.6	36.6	36.9	36.9	37.2	37.2	37.4	18.4
Correlation	−0.47	−0.79	−0.84	−0.83	−0.85	−0.83	−0.78	−0.77	−0.75	−0.75	−0.76	−0.77	−0.26	−0.28
Threshold = +1.5														
Mean #	63.1	39.0	23.8	12.8	7.1	5.0	3.8	3.1	2.7	2.4	2.3	2.0	1.9	27.1
Mean length	3.7	7.1	12.6	24.7	47.9	70.6	94	114.7	133.8	153.1	168.4	188.3	133	7.1
% of time	18.0	21.0	22.8	23.8	25.3	25.7	26.1	26.2	26.6	26.7	27.2	27.3	27.7	12.7
Correlation	−0.43	−0.66	−0.70	−0.68	−0.75	−0.69	−0.64	−0.62	−0.63	−0.64	−0.65	−0.67	−0.16	−0.23
Threshold = +2.0														
Mean #	21.8	15.5	9.9	5.6	3.3	2.4	1.9	1.6	1.5	1.4	1.3	1.2	1.2	19.4
Mean length	3.9	7.9	14.5	29	56.8	82.2	108.0	128.3	146.8	164	178.9	195.3	132.8	6.5
% of time	6.5	9.2	10.8	12.1	13.6	14.2	15.0	15.4	16.2	17.1	17.9	18.9	20.1	8.1
Correlation	−0.30	−0.39	−0.44	−0.45	−0.46	−0.42	−0.40	−0.37	−0.35	−0.35	−0.35	−0.36	−0.10	−0.12
Threshold = +3.0														
Mean #	1.7	1.5	1.3	1.1	1.0	1.0	1.0	1.0	1.0	1.1	1.0	1.0	1.0	7.9
Mean length	3.9	8.4	16.9	33.2	64.1	88.9	104.7	120.1	136.3	138.7	147.5	151.0	119.5	5.5
% of time	0.5	1.0	1.6	2.9	5.2	7.1	8.4	9.6	11.0	11.3	12.2	12.6	13.3	2.8
Correlation	−0.07	−0.06	−0.03	−0.03	−0.06	−0.05	−0.05	0.00	−0.03	−0.01	0.00	0.00	0.00	0.09

total number of months a grid point was in an event divided by the entire 108-year record (1296 months). A simple Pearson correlation was calculated on the basis of the association between the number of events and the length of each event for each grid cell. Table V shows the summary statistics for all 14 indices and 10 thresholds.

More events would be expected with short timescales such as the 1-, 3- and 6-month SPI, and low thresholds such as ±0.5. The statistics in Table V show this result.

DOI: 10.1002/joc

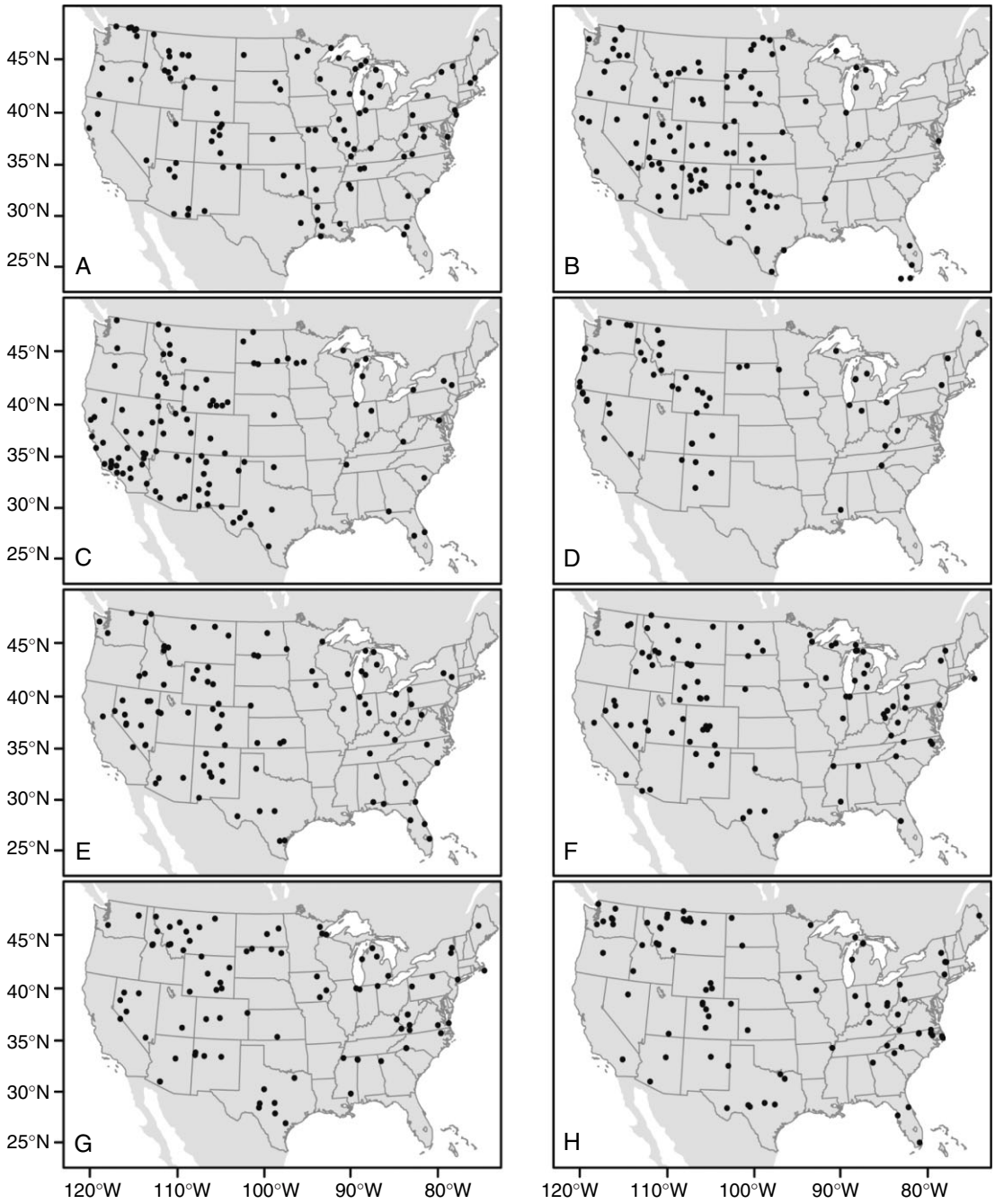

Figure 15. Maps showing the locations (solid dot symbol) of the most extreme annual dry values for the 1895–2003 period for (A) 1-month SPI, (B) 3-month SPI, (C) 6-month SPI, (D) PDSI, (E) 12-month SPI, (F) 24-month SPI, (G) 36-month SPI and (H) 72-month SPI.

The mean length of events is maximized with the long timescales and high thresholds (±2) for both positive and negative precipitation anomalies. The mean length column shows that increasing event length corresponds to increasing index timescale.

The percent of time spent in an anomalous precipitation event is related to the threshold used to define the event. Lower thresholds have a greater percent of time in an anomalous precipitation event. Soulé (1992) determined that, since the different Palmer values have different timescales, it is possible for an area to have near normal agricultural productivity, while at the same time experiencing a major hydrological or meteorological drought. This is because the shorter timescale droughts such as agricultural PDSI often have one or more months of normal or above-normal precipitation during a longer-term hydrologic drought. These few months are enough to return the index to greater than zero for a few months, thus ending the short-term agricultural drought but not ending the long-term hydrologic drought. The same evidence is provided in Table V using SPI indices. With a threshold of −0.5, the mean length of a drought is 3 months using the 1-month SPI, but 15 months using the 12-month SPI. Therefore, many droughts could start and stop using the 1-month SPI in the amount of time an average 12-month SPI drought started and stopped.

DOI: 10.1002/joc

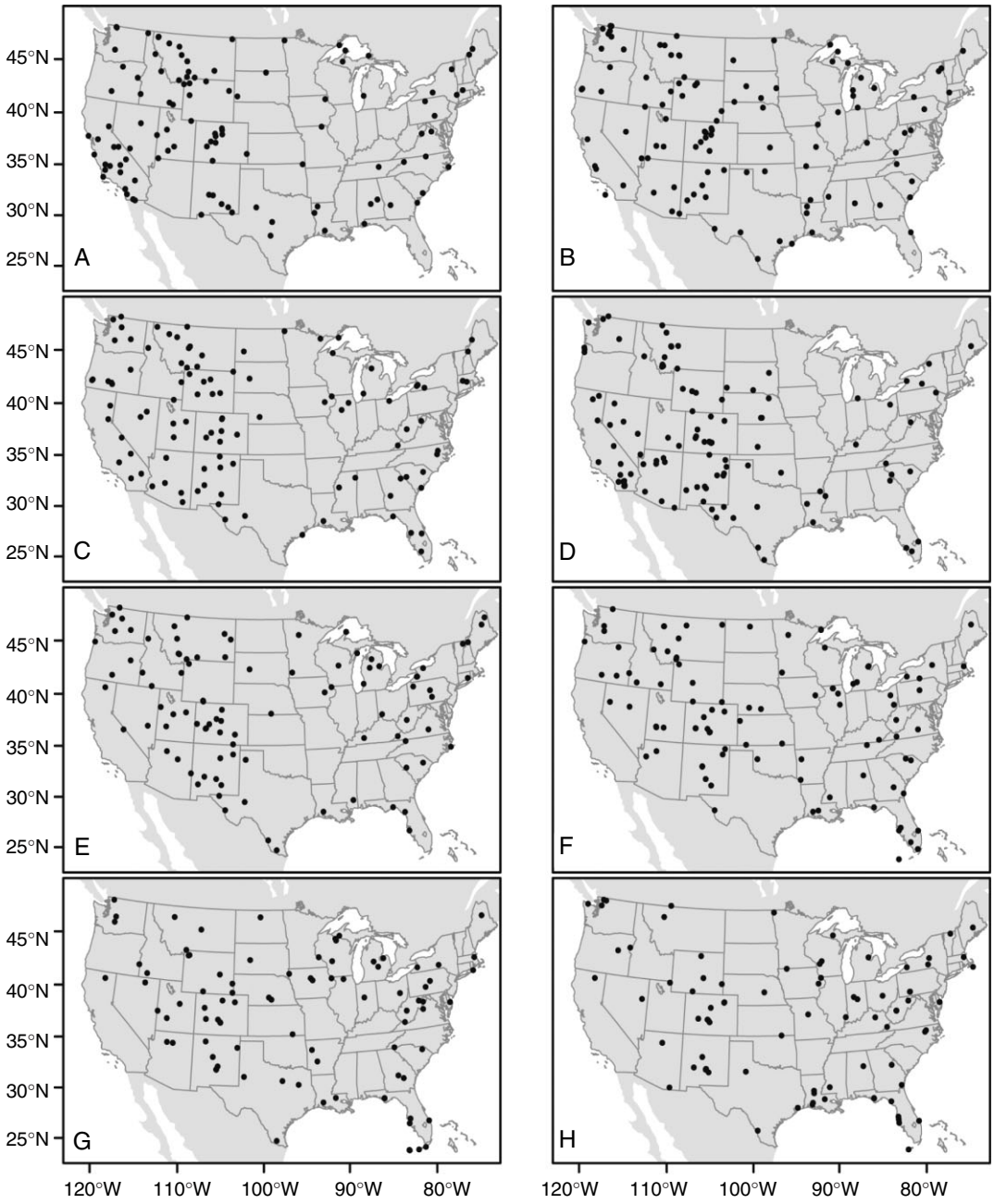

Figure 16. Same as Figure 15 except for most extreme annual wet values.

This was also seen with the time series of drought areas (Figure 5) where the shorter timescales would have numerous peaks over the same time period as one wider peak in the longer timescales.

Soulé (1992) also states that there should be a negative relationship between the number of droughts and duration. An increase in duration would reduce the opportunity for new drought or wet events to be recorded. A simple correlation shows this is true when the threshold values are low (i.e., ± 0.5 or ± 1) with the exception of the 1-month SPI given correlations of -0.8 and -0.7. For example, with the 6-month SPI and a -0.5 threshold, the correlation is 0.89 between the number of drought events and the length of drought events. When thresholds are increased to -2 or greater, there seems to be a much smaller, if any, relationship between the number of events and duration.

SUMMARY AND CONCLUSIONS

The purpose of this study was to examine the spatial and temporal characteristics of drought and pluvial events utilizing a monthly US high-resolution (4-km) spatial dataset for the period 1895–2003. A number of timescales, indices (SPI and PDSI) and thresholds were used in the analysis. Some of the resulting temporal and spatial patterns were not surprising and concurred with previous studies. For example, indices with longer timescales also had longer duration events, while

DOI: 10.1002/joc

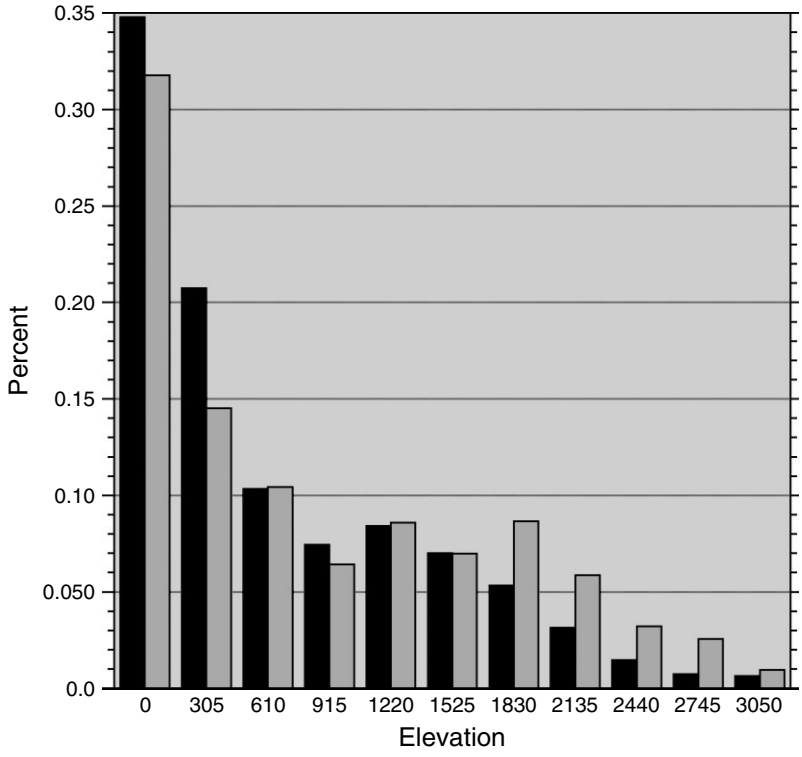

Figure 17. Frequency histogram of elevations for the drought and pluvial extremes (gray) plotted with the elevations of all 451 709 grid points used in the analysis (black). Elevations are in meters.

shorter timescales had shorter and more frequent events. SPI patterns at 1- and 3-month timescales showed that drought and pluvial are more prevalent in the interior United States compared to coastal areas.

The definition of a drought or pluvial in terms of index magnitude can dramatically affect the size, duration and location of the event. Indices with short timescales exhibit substantial intraseasonal variability in both size and area, while longer timescales are more persistent and vary slowly. The longer timescales show no single area of the country especially prone to having a higher occurrences of large anomalous precipitation areas (unlike the short timescale indices). It is common for an area to be under drought conditions at one timescale and normal or anomalous wet at another timescale and vice versa. This highlights the importance of using multiple indices when possible or using the appropriate timescales when analyzing and assessing moisture anomalies.

Summary statistics from the study indicate a greater number of droughts with shorter timescales and lower (i.e., ± 0.5 or ± 1) thresholds, and that the longest droughts occur with the lowest thresholds and longest timescales. Correlations show a strong relationship between the number of anomalous precipitation events and duration. The highest correlations occur for index thresholds between ± 1; very low correlations occurred for thresholds exceeding ± 2.

Soulé (1992) found that when increasing the resolution from statewide averaged precipitation to climate divisions, the basic trends remained the same but the divisions showed less homogenous patterns. As expected, the 4-km PRISM data used in this study showed a much greater level of detail than divisional data. Though the general patterns remain the same, the higher resolution data shows for many cases areas considerably less homogenous than for climate divisions.

Analysis of drought areas indicates that short-term droughts exhibit substantial temporal and spatial variability. It is not uncommon for large areas to be in drought conditions for 1 month but not during the next month. On the other hand, as the timescales are lengthened, more persistent droughts become evident. For example, the 12-month SPI begins to clearly show the three peaks of the 1930s drought. The 24-month SPI and longer timescales clearly show that the 1930s and 1950s were the largest and longest droughts in the 108-year period analyzed. Pluvials have similar characteristics to changing timescales.

A previous study by Fye *et al*. (2003) showed that 1905–1917 was the largest and most persistent pluvial in at least recorded history. However, the results here showed that there were at least three periods of similar length after 1970 in which a greater portion of the country was experiencing a pluvial. A 1973–1981 pluvial occurred over the eastern United States, a 1983–1988 pluvial extended over much of the West and a 1990–2000 pluvial covered much of the country but persisted longest in the central and southern United States.

The use of high-resolution (4-km) data in this study verified the patterns of previous studies, but showed that areas of anomalous precipitation contain greater detail than seen using climate division data. The drought

DOI: 10.1002/joc

patterns matched closely with those of previous studies whereas the pluvials showed an increase in occurrence throughout the United States since 1970, a pattern only briefly mentioned in some papers. The results showed that large and long-lasting pluvials have occurred three times in the past 30 years. The largest drought and pluvial areas also occurred more frequently during the winter months, specifically December and January. While the central United States was the most prominent for large drought and pluvials, the most extreme values occurred more regularly in the West and to some extent in the East. Many of the western extremes occurred at high elevations raising a question of whether these are physically based upon a persistent synoptic scale pattern or an artifact of high-elevation PRISM data.

A comparison of the spatially high-resolution indices to climate divisions suggests that there can be substantial differences in index magnitude. In theory, PRISM should be especially relevant across the complex terrain and elevation differences across the western United States. However, it is easy to find substantial differences between PRISM values within a climate division and independently computed divisional values. This may or may not be of relevance to a researcher or practitioner depending upon whether or not the interest is a coarse representation of an area or increased detail.

ACKNOWLEDGEMENTS

We thank Chris Daly for making the PRISM data possible and for providing initial advice to us. Greg McCurdy at the WRCC provided valuable information and insight regarding the SPI and PDSI indices and Fortran code. We thank Hauss Reinbold and Beth Hall for providing software and graphics assistance, and manuscript comments. Thanks are also due to Jeff Underwood and John Lewis for their support of this work, as well as their recommendations and feedback. The comments of the anonymous reviewers are also appreciated. This work was supported by the Bureau of Land Management National Office of Fire and Aviation under cooperative Assistance Agreement number 1422RAA000002.

REFERENCES

Allen GD, Breshears DD. 1998. Drought-induced shift of a forest-woodland ecotone: rapid landscape response to climate variation. *Ecology* **95**: 14839–14842.

Alley WM. 1984. The palmer drought severity index: limitations and assumptions. *Journal of Applied Meteorology* **23**: 1100–1109.

Alley WM. 1985. The palmer drought severity index as a measure of hydrologic drought. *Water Resources Bulletin* **21**: 104–114.

Bark LD. 1978. *History of American Droughts*. Westview Press: Boulder, CO.

Binford MW, Kolata AL, Brenner M, Janusek JW, Seddon MT, Abbot M, Curtis JH. 1997. Climate variation and the rise and fall of an Andean civilization. *Quaternary Research* **47**: 235–248.

Bordi I, Sutera A. 2004. Drought variability and its climatic implications. *Global and Planetary Change* **4**: 115–127.

Bordi I, Frigio S, Parenti P, Speranza A, Sutera A. 2001. The analysis of the standardized precipitation index in the mediterranean area: part 1. *Annali di Geofisica* **44**: 965–978.

Bowden MJ, Kates RW, Kay PA, Riebsame WE, Warrick RA, Johnson DL, Gould HA, Weiner D. 1981. The effect of climate fluctuations on human populations: two hypothesis. In *Climate and History: Studies of Past Climates and Their Impacts on Man*, Wrigley TML, Ingram MJ, Farmer G (eds). Cambridge University Press: Cambridge, UK; 479–513.

Carr JR. 2002. *Data Visualization in the Geosciences*. Prentice Hall: Englewood Cliffs, NJ; 267.

Dale VH, Joyce LA, McNulty S, Neilson RP, Ayres MP, Flannigan MD, Hanson PJ, Irland LC, Lugo AE, Peterson CJ, Simberloff D, Swanson FJ, Stocks BJ, Michael WB. 2001. Climate change and forest disturbances. *Bioscience* **51**: 723–734.

Daly C, Neilson RP, Phillips DL. 1994. A statistical-topographic model for mapping climatological precipitation over mountainous terrain. *Journal of Applied Meteorology* **33**: 140–158.

Daly C, Taylor G, Gibson W. 1997. The PRISM approach to mapping precipitation and temperature. Preprints *10th Conference on Applied Climatology*. American Meteorological Society; Boston, MA 10–12.

Diaz HF. 1983. Drought in the United-States–Some aspects of major dry and wet periods in the contiguous United-States, 1895–1981. *Journal of Climate and Applied Meteorology* **22**: 3–16.

Fye FK, Stahle DW, Cook ER. 2003. Paleoclimatic analogs to twentieth-century moisture regimes across the United States. *Bulletin of the American Meteorological Society* **84**: 901–909.

Guttman NB. 1997. Comparing the palmer drought index and the standardized precipitation index. *Journal of the American Water Resources Association* **34**: 113–121.

Guttman NB. 1999. Accepting the standardized precipitation index: a calculation algorithm. *Journal of the American Water Resources Association* **35**: 311–322.

Hanson PJ, Weltzin JF. 2000. Drought disturbance from climate change: response of United States forests. *Science of the Total Environment* **262**: 205–220.

Haug GH, Gunther D, Peterson LC, Sigman DM, Hughen KA, Aeschlimann B. 2003. Climate and the collapse of Maya civilization. *Science* **299**: 1731–1735.

Hayes MJ, Svoboda MD, Wilhite DA, Vanyarkho OV. 1999. Monitoring the 1996 drought using the standardized precipitation index. *Bulletin of the American Meteorological Society* **80**: 429–438.

Heim RR. 2002. A review of twentieth-century drought indices used in the United States. *Bulletin of the American Meteorological Society* **83**: 1149–1165.

Hidalgo HG. 2004. Climate precursors of multidecadal drought variability in the western United States. *Water Resources Research* **40**: W12504.

Karl TR. 1983. Some spatial characteristics of drought duration in the United-States. *Journal of Climate and Applied Meteorology* **22**: 1356–1366.

Karl TR. 1986. The sensitivity of the palmer drought severity index and palmer's Z-index to their calibration coefficients including potential evapotranspiration. *Journal of Applied Meteorology* **25**(1): 77–86.

Karl TR, Koscielny AJ. 1982. Drought in the United States: 1895–1981. *Journal of Climatology* **2**: 313–329.

Karl TR, Knight RW. 1985. *Atlas of Monthly Palmer Hydrological Drought Indices (1931–1983) for the Contiguous United States*. National Climatic Data Center Historical Climatology Series 3–7: Ashville, NC; 319.

Karl TR, Quinlan F, Ezell DS. 1987. Drought termination and amelioration: its climatological probability. *Journal of Climate and Applied Meteorology* **26**: 1198–1209.

Karl TR, Knight RW, Easterling DR, Quaye RG. 1996. Indices of climate change for the United States. *Bulletin of the American Meteorological Society* **77**: 279–292.

Klugman MR. 1978. Drought in the upper Midwest, 1931–1969. *Journal of Applied Meteorology* **17**: 1425–1431.

Lenihan JM, Drapek R, Bachelet D, Neilson RP. 2003. Climate change effects on vegetation distribution, carbon, and fire in California. *Ecological Applications* **13**: 1667–1681.

McGregor KM. 1985. Drought during the 1930s and 1950s in the central United States. *Physical Geography* **6**: 288–301.

McKee TB, Doesken NJ, Kleist J. 1993. The relationship of drought frequency and duration to time scales. Preprints *Eighth Conference on Applied Climatology*. American Meteorological Society: Boston, MA; 179–184.

McKee TB, Doesken NJ, Kleist J. 1995. Drought monitoring with multiple-time scales. Preprints *Ninth Conference on Applied Climatology*. American Meteorological Society: Boston, MA; 233–236.

DOI: 10.1002/joc

Miller DA, White RA. 1998. A conterminous United States multilayer soil characteristics dataset for regional climate and hydrology modeling. *Earth Interactions* **2**: 1–26.
Oladipo EO. 1986. Spatial patterns of drought in the interior plains of North America. *Journal of Climatology* **6**: 495–513.
Palmer WC. 1965. *Meteorological Drought*, *Research Paper No. 45*. U.S. Weather Bureau: Washington, DC; 58.
Redmond KT. 2002. The depiction of drought: a commentary. *Bulletin of the American Meteorological Society* **83**: 1143–1147.
Riebsame WE, Changnon SA, Karl TR. 1991. *Drought and Natural Resource Management in the United States: Impacts and Implications of the 1987-89 Drought*. Westview Press: Boulder, CO; 174.
Rogers GF, Vint MK. 1987. Winter precipitation and fire in the Sonoran desert. *Journal of Arid Environments* **13**: 47–52.
Skaggs RH. 1975. Drought in the United States, 1931–1940. *Annual Association of American Geography* **65**: 391–402.
Soulé PT. 1992. Spatial patterns of drought frequency and duration in the contiguous USA based on multiple drought event definitions. *International Journal of Climatology* **12**: 11–24.
Soulé PT, Meentemeyer V. 1989. The drought of 1988: historical rank and recurrence interval. *Southeastern Geography* **29**: 17–25.
Steila D. 1972. *Drought in Arizona*. University of Arizona, Division of Economic and Business Research: Tucson; 78.
Steinemann A. 2003. Drought indicators and triggers: a stochastic approach to evaluation. *Journal of the American Water Resources Association* **39**: 1217–1232.
Swetnam TW, Betancourt JL. 1998. Mesoscale disturbance and ecological response to decadal climatic variability in the American Southwest. *Journal of Climate* **11**: 3128–3147.
Thornthwaite CW. 1948. An approach towards a rational classification of climate. *Geographical Review* **38**: 55–94.
Walsh JE, Richman MB, Allen DW. 1982. Spatial coherence of monthly precipitation in the United States. *Monthly Weather Review* **110**: 272–286.
Weiss B. 1981. The decline of a late bronze age civilization as a possible response to climate change. *Climate Change* **4**: 173–198.
Willeke G. 1994. *The National Drought Atlas*. Institute for Water Resources REP. 94-NDS-4, U.S. Army Corps of Engineers: Fort Belvoir, VA; 587.
Woodhouse CA, Overpeck JT. 1998. 2000 years of drought variability in the Central United States. *Bulletin of the American Meteorological Society* **79**: 2693–2714.
Yevjevich V. 1967. *An Objective Approach to Definitions and Investigations of Continental Drought*, *Hydrology Papers, No. 23*. Colorado State University: Fort Collins, CO; 19.

DOI: 10.1002/joc